

# Recent Advances in Microgels: From Biomolecules to Functionality

Yufan Xu, Hongjia Zhu, Akhila Denduluri, Yangteng Ou, Nadia A. Erkamp, Runzhang Qi, Yi Shen,\* and Thomas P. J. Knowles\*

The emerging applications of hydrogel materials at different length scales, in areas ranging from sustainability to health, have driven the progress in the design and manufacturing of microgels. Microgels can provide miniaturized, monodisperse, and regulatable compartments, which can be spatially separated or interconnected. These microscopic materials provide novel opportunities for generating biomimetic cell culture environments and are thus key to the advances of modern biomedical research. The evolution of the physical and chemical properties has, furthermore, highlighted the potentials of microgels in the context of materials science and bioengineering. This review describes the recent research progress in the fabrication, characterization, and applications of microgels generated from biomolecular building blocks. A key enabling technology allowing the tailoring of the properties of microgels is their synthesis through microfluidic technologies, and this paper highlights recent advances in these areas and their impact on expanding the physicochemical parameter space accessible using microgels. This review finally discusses the emerging roles that microgels play in liquid–liquid phase separation, micromechanics, biosensors, and regenerative medicine.

## 1. Introduction

Microgels have been developed as biomaterials for many applications, especially in medical engineering and drug delivery, due to their miniaturized size, versatile compositions, flexible structures, and high biodegradability.<sup>[1–7]</sup> Homogeneous microgels have constant composition and gel density throughout the microgels; spatially inhomogeneous microgels have varying density of the gel materials; heterogeneous microgels have varied composition of gel materials.<sup>[3,4,8]</sup> While the homogeneous microgels have been used as 3D scaffold models for cell growth, inhomogeneous and heterogeneous microgels can more accurately mimic the physiological environment in vivo.<sup>[3,9–11]</sup> By exploiting microfluidic platforms, microgels can be produced with controlled size, shape, structures, and compositions.<sup>[12–17]</sup> In particular, microgels with inhomogeneous compositions and heterogeneous structures can be realized


by microfluidic approaches by controlling the flow. The size of microgels usually ranges from 1  $\mu\text{m}$  to several hundred  $\mu\text{m}$ ;<sup>[2–4,8]</sup> nanogels (from several tens of nm) are sometimes called microgels in the literature.<sup>[18–24]</sup> In this review, we discuss microgels with different morphologies, materials, and applications including those with homogeneous and inhomogeneous compositions as well as heterogeneous structures. We also provided an overview of the fabrication systems, characterization methods, and their biological applications such as liquid–liquid phase separation (LLPS), micromechanics, biosensing, and 3D cell culture.

Homogeneous microgels with structures of spheres,<sup>[3]</sup> tear drops,<sup>[14,25]</sup> hole shells,<sup>[26]</sup> rods,<sup>[1,11,27–29]</sup> and raspberry-like shapes,<sup>[30]</sup> have been fabricated using microfluidics (Figure 1). For more versatile functions, inhomogeneous microgels with core-shell,<sup>[3,8,14,31–33]</sup> compartmentalized,<sup>[34]</sup> and Janus<sup>[8,35–37]</sup> structures have been developed (Figure 1). As a result of the geometry, the surface to volume ratio of microgels is higher than that of bulk gels.<sup>[3]</sup> The interface interaction between the gel and the surrounding medium, the gel/oil, gel/sol, gel/water, gel/gel, and even gel/cell interface, can make a difference to the morphology of the microgels (Figure 1).<sup>[2,4,8,28,38]</sup> These interfaces could be sites where chemical reactions take place at the microscale, or be barriers in the contexts of molecule or particle migration. Both the interfaces and the microgel bodies can act as microreactors for the high-throughput drug discovery and test.<sup>[39–43]</sup>

Y. Xu, H. Zhu, A. Denduluri, Y. Ou, N. A. Erkamp, R. Qi, Y. Shen,  
T. P. J. Knowles  
Centre for Misfolding Diseases  
Yusuf Hamied Department of Chemistry  
University of Cambridge  
Cambridge CB2 1EW, UK  
E-mail: yi.shen@sydney.edu.au; tpjk2@cam.ac.uk

Y. Shen  
School of Chemical and Biomolecular Engineering  
The University of Sydney  
Sydney, NSW 2006, Australia  
Y. Shen  
The University of Sydney Nano Institute  
University of Sydney  
Sydney, NSW 2006, Australia

T. P. J. Knowles  
Cavendish Laboratory  
University of Cambridge  
Cambridge CB3 0HE, UK

 The ORCID identification number(s) for the author(s) of this article can be found under <https://doi.org/10.1002/smll.202200180>.

© 2022 The Authors. Small published by Wiley-VCH GmbH. This is an open access article under the terms of the Creative Commons Attribution License, which permits use, distribution and reproduction in any medium, provided the original work is properly cited.

DOI: 10.1002/smll.202200180

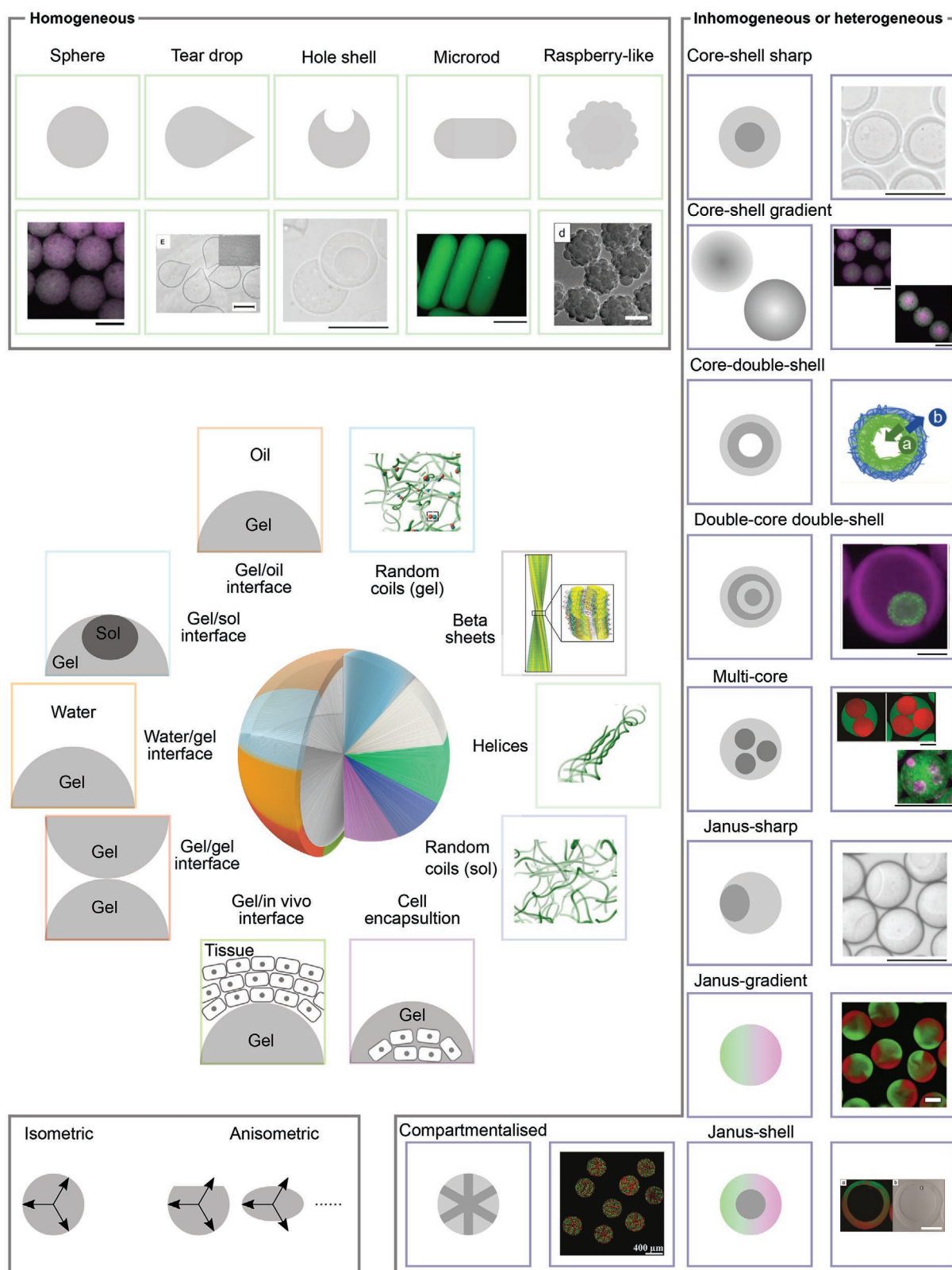


**Figure 1.** Microgels with different morphologies or structures, such as spheres,<sup>[3]</sup> tear-drop,<sup>[57]</sup> hole-shell,<sup>[8]</sup> core-shell,<sup>[3,8,33]</sup> Janus,<sup>[8,36,37]</sup> compartmentalized,<sup>[34]</sup> rod,<sup>[4]</sup> and raspberry-like shapes.<sup>[30]</sup> Scale bars = 200  $\mu\text{m}$  (tear-drop), 500  $\mu\text{m}$  (microrod), 0.3  $\mu\text{m}$  (submicron, raspberry-like), 400  $\mu\text{m}$  (compartmentalized), and 100  $\mu\text{m}$  (all other). The microgel/environment interfaces can include gel/oil,<sup>[1,3]</sup> gel/sol,<sup>[8]</sup> gel/water,<sup>[3,4]</sup> gel/gel,<sup>[33]</sup> and gel/tissue interfaces.<sup>[34,341]</sup> The internal structures of the building blocks can be random coils,<sup>[3]</sup> alpha helices,<sup>[3]</sup> beta sheets,<sup>[339]</sup> etc. Reproduced under the

Microgels with a range of shapes can be applied to different functional applications. Spherical microgels (isometric) are the most common form of microgels, as a result of interfacial tension.<sup>[2,3]</sup> In 3D cell culture, such isometric microgels allow the uniform exchange or diffusion of nutrients and metabolic wastes.<sup>[2,3]</sup> In contrast, the distance from the geometric center to the surface can vary in anisometric microgels such as micro-rods, resulting in different diffusion of substances along the radial and axial directions.<sup>[11,28,44]</sup> The hole-shell microgels have both convex and concave surfaces, and this combined curvature can be applied to lock-and-key structures as intelligent joints.<sup>[8,45–47]</sup> Tear-drop microgels and spherical microgels have demonstrated different release profiles of molecules.<sup>[48]</sup> Core-shell or hollow microgels can have different materials or payloads at specific microgel positions.<sup>[8,49]</sup> For example, controllable degradability or stiffness of microgels can be achieved by adopting different materials at the core and near shell.<sup>[8,49]</sup> Heterotypic cells can be encapsulated at the core and shell to fulfill biomimetic functions of the microgels.<sup>[50,51]</sup> Janus and multicompartimentalized microgels, in addition, are promising platforms to generate and nurture multicellular segmented tissues.<sup>[34,52]</sup>

Microgels can be assembled from a series of elementary building blocks, including nonbiological macromolecules, colloids, and biomolecules.<sup>[2,3,53,54]</sup> In this review, we focus on microgels assembled from biomolecules; by using naturally occurring or in some cases biomimetic building blocks, unique advantages in terms of biocompatibility and ability to interface with biological systems can be generated. Microgels can be formed from cross-linked biomolecules or from supramolecular assemblies of such biomolecules, including protein nanofibrils.<sup>[55,56,57]</sup> By assembling microgels with building blocks at different scales, controlled release of drug molecules and desired mechanical properties can be achieved.<sup>[58]</sup> The assembly can be modulated by the flow patterns in the microfluidic devices and cross-linking methods. For example, microgels with a core-shell structure have been prepared by coflowing gelatin and other aqueous solutions in a microfluidic channel through both physical and chemical gelation regimes.<sup>[3,8]</sup> Using this production method, microgels can be produced with specific morphology and drug release rate, making them both relevant systems for drug release and in vivo implants.

Here, we discuss recent multifaceted research progress in microgels in the fields of novel biomedical technologies rooted in materials and engineering science, such as LLPS (**Figure 2**), micromechanics (**Figure 3**), biosensors (**Figure 4**), and regenerative medicine (**Figure 5**). Representative morphologies and compositions of the microgels are introduced (**Figure 1**). The fabrication of the microgels is discussed; in particular, we will focus on hydrogel materials (**Table 1**), categories of microfluidic

or nonmicrofluidic methods (**Figure 6**), surfactants, and demulsification (**Tables 2 and 3**). Some key characterization methods for microgels are discussed (**Figure 7 and Table 4**). Finally, we share our outlook of the use of microgels in emerging fields. This review is expected to cast light on the development of hydrogels at the microscale and sets out to assist and inspire researchers interested in microgels for biomedical and bioengineering purposes.

## 2. Anisometric Microgels for All-Aqueous LLPS

Microgels can be formed from LLPS systems and can reversibly switch from gel states to liquid states.<sup>[4,53]</sup> Recent work shows that anisometric protein microrod gels can be applied to the engineering of a highly monodisperse aqueous LLPS system (**Figure 2a**).<sup>[4]</sup> Through the thermo-induced gel-sol transition (reversing cross-linking) of gelatin, the water/water interfacial tension becomes the dominant energetic contribution as elasticity diminishes.<sup>[4]</sup> In addition, the fusion of protein phases has been observed during the gel-sol transition of rod microgels.<sup>[4]</sup> This fusion phenomenon complements previous studies<sup>[59–62]</sup> on the coalescence of liquid droplets. Isometric microgels can also function as precursors of all-aqueous LLPS systems, though these microgels do not display the rod-to-sphere shape change.<sup>[4]</sup> It is worth mentioning that all-aqueous LLPS systems and aqueous two-phase systems can overlap to some extent.<sup>[63,64]</sup>

Hole-shell microgels and buckled core-shell microgels, can also function as precursors and indicators of all-aqueous LLPS systems that are biphasic or multiphasic (**Figure 2b,c**).<sup>[8]</sup> Similar to rod microgels, the morphological evolution of hole-shell microgels and the fusion of the hole-shell microgels in crowders can characterize LLPS.<sup>[8]</sup> Furthermore, multiphase all-aqueous LLPS systems can be achieved by reversing the cross-linking of buckled core-shell microgels in crowders.<sup>[8]</sup> Buckled core-shell microgels transform into spherical core-shell droplets, indicating the liquid nature of the all-aqueous LLPS systems.<sup>[8]</sup> More intriguingly, the fusion of such spherical core-shell droplets is clearly demonstrated by the shell-shell fusion followed by the core-core fusion of two condensates,<sup>[8]</sup> which can be promising models of multiphase or vesicle-like condensates from other materials.

LLPS of biomolecules can have implications on functional and aberrant biology, as well as on the processing and designing of multifunctional and smart biomaterials.<sup>[59,60,65–69]</sup> Most of the existing LLPS studies have focused on the sol-gel transition (liquid-to-solid) transition of the condensates, as the gel or aggregation outcomes are thought to be related to the onset and development of protein aggregation diseases.<sup>[55,59,60,67]</sup>

terms of the Creative Commons CC BY license.<sup>[1]</sup> Copyright 2017, The Authors, published by Springer Nature; Reproduced under the terms of the Creative Commons CC BY license.<sup>[3]</sup> Copyright 2020, The Authors, published by WILEY-VCH; Reproduced under the terms of the Creative Commons CC BY license.<sup>[4]</sup> Copyright 2021, The Authors, published by WILEY-VCH; Reproduced under the terms of the Creative Commons CC BY license.<sup>[8]</sup> Copyright 2021, The Authors, published by WILEY-VCH; Reproduced with permission.<sup>[57]</sup> Copyright 2021, WILEY-VCH; Reproduced with permission.<sup>[30]</sup> Copyright 2014, American Chemical Society; Reproduced with permission.<sup>[33]</sup> Copyright 2010, American Chemical Society; Reproduced with permission.<sup>[36]</sup> Copyright 2010, Elsevier; Reproduced with permission.<sup>[37]</sup> Copyright 2010, American Chemical Society; Reproduced with permission.<sup>[34]</sup> Copyright 2021, WILEY-VCH; Reproduced with permission.<sup>[339]</sup> Copyright 2013, National Academy of Sciences; Reproduced with permission.<sup>[341]</sup> Copyright 2020, Royal Society of Chemistry.

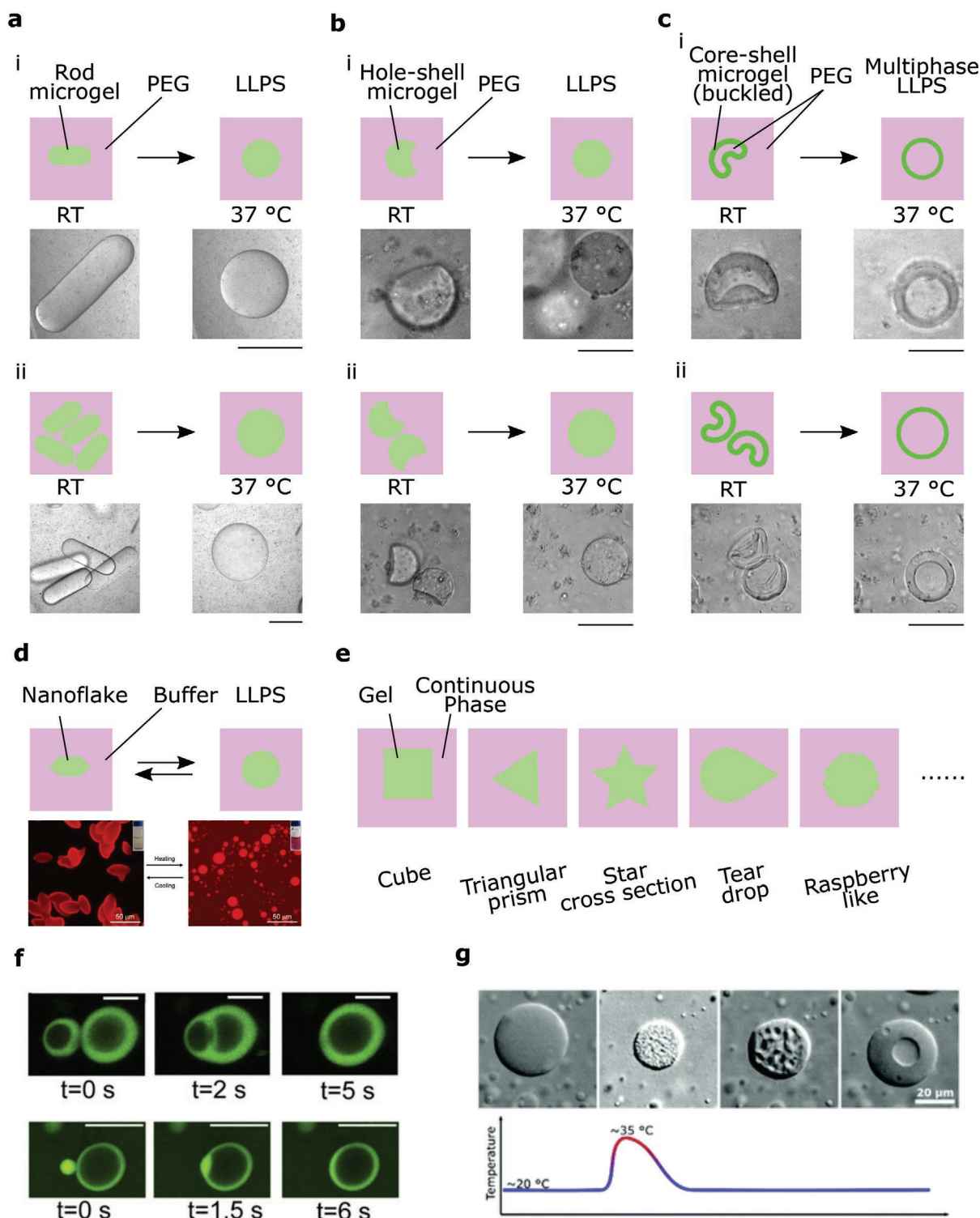


**Figure 2.** Anisometric microgels as precursors and indicators of all-aqueous liquid-liquid phase-separated systems. a–c) Engineered anisometric gelatin microgels function as precursors of all-aqueous liquid-liquid phase-separated systems, through the thermo-induced gel-sol transition of gelatin in a macromolecular crowding. Rod (a), hole-shell (b), and buckled core-shell (c) microgels are demonstrated here. Scale bars = 500  $\mu\text{m}$  (a), 50  $\mu\text{m}$  (b(i),c(i)), and 100  $\mu\text{m}$  (b(ii),c(ii)). Reproduced under the terms of the Creative Commons CC BY license.<sup>[4]</sup> Copyright 2021, The Authors, published by WILEY-VCH; Reproduced under the terms of the Creative Commons CC BY license.<sup>[8]</sup> Copyright 2021, The Authors, published by WILEY-VCH. d) Temperature-induced phase transition from co-assembled nanosheets to liquid droplets. Scale bars = 50  $\mu\text{m}$ . Reproduced with permission.<sup>[60]</sup> Copyright 2020, WILEY-VCH. e) Potential examples of other nonspherical or anisometric microgels as precursors and indicators of all-aqueous liquid-liquid phase-separated systems. The microgel morphologies can be cubes,<sup>[46]</sup> triangular prisms,<sup>[74]</sup> star cross-sectioned,<sup>[127]</sup> tear drops,<sup>[25]</sup> raspberry-like,<sup>[72]</sup>

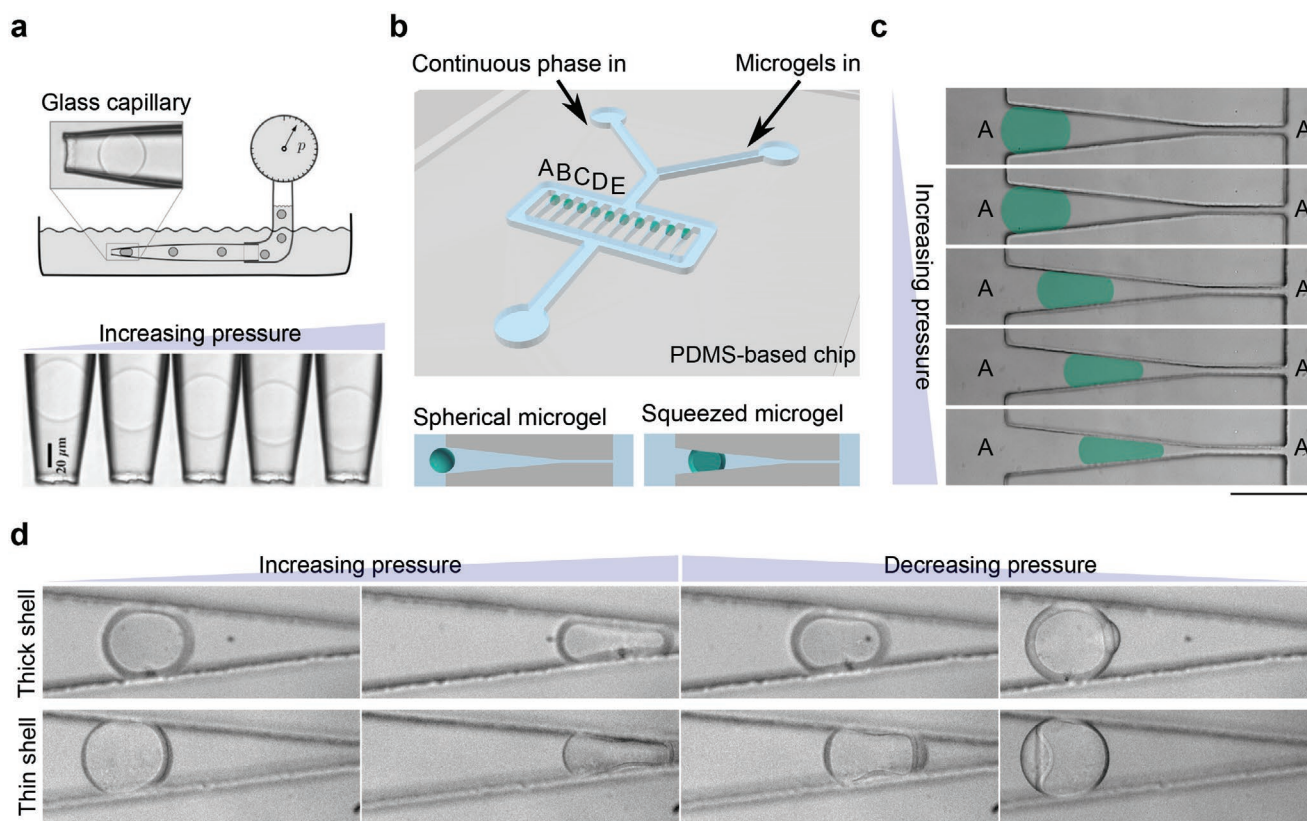


**Figure 3.** Microfluidic testing of the micromechanics of soft microgels. a) A glass-capillary device that has one tapering channel for the mechanical testing of soft microgels. Scale bar = 20  $\mu\text{m}$ . Reproduced with permission.<sup>[86]</sup> Copyright 2010, Royal Society of Chemistry. b) A PDMS-based device with parallel tapering channels for mechanical testing of multiple soft solid microgels. Reproduced under the terms of the Creative Commons CC BY license.<sup>[87]</sup> Copyright 2022, The Authors, published by Springer Nature. c) A microgel trapped in one of the channels (b) deforms with increasing flow rate of the continuous aqueous phase. Scale bar = 200  $\mu\text{m}$ . Reproduced under the terms of the Creative Commons CC BY license.<sup>[87]</sup> Copyright 2022, The Authors, published by Springer Nature. d) A core-shell microgel trapped in one of the channels (b) buckles with fluctuating flow rate of the continuous oil phase.<sup>[8]</sup> Scale bar = 100  $\mu\text{m}$ . Reproduced under the terms of the Creative Commons CC BY license.<sup>[8]</sup> Copyright 2021, The Authors, published by WILEY-VCH.

However, the gel-sol transition, that is, the reversing of the cross-linking, has not been well studied in detail because of the following challenges. A practical challenge is the lack of a scalable approach to rapidly producing monodisperse liquid-liquid systems. A conceptual challenge is that liquid (proteinaceous) materials have not been widely applied as a class of functional materials yet.<sup>[4,70]</sup> Liquid materials have advantages in terms of processibility due to their liquid nature relative to solid or semisolid materials, and are expected to open up new possibilities for biomedical research in liquids.<sup>[4,70]</sup> The abovementioned anisometric microgels are examples of generating all-aqueous LLPS systems with size-controllable and heterogeneity-tunable condensates.<sup>[4,8]</sup> Gel-sol transition of nonprotein materials has also been recently demonstrated; nanosheets of porphyrin/ionic-liquid co-assembly have been found to be the outcomes

and the precursors of LLPS (Figure 2d).<sup>[60]</sup> The nanosheet-to-sphere morphological change and the fusion of the solute-rich phases can highlight the liquid nature of the dispersed condensates.<sup>[60]</sup> We envision that other nonspherical or anisometric nano/microgels from diverse materials with multiple fabrication methods, can act as precursors and indicators of all-aqueous LLPS systems (Figure 2e).<sup>[25,28,46,71–75]</sup>

Two different types of heterogeneity have so far been observed in spontaneously formed condensates. Multiphase condensates contain multiple phases or regions with different contents. These subcompartments have been observed in cells in stress granules, paraspeckles, nuclear speckles, and nuclei.<sup>[76–79]</sup> To better understand this behavior, in vitro model systems have been made with proteins and optionally nucleic acids.<sup>[80,81]</sup> Multiphase condensates are now understood to have

etc. Reproduced with permission.<sup>[46]</sup> Copyright 2008, National Academy of Sciences; Reproduced with permission.<sup>[74]</sup> Copyright 2016, WILEY-VCH; Reproduced with permission.<sup>[127]</sup> Copyright 2015, Springer Nature; Reproduced with permission.<sup>[25]</sup> Copyright 2015, Elsevier; Reproduced under the terms of Creative Commons CC BY license.<sup>[72]</sup> Copyright 2018, The Authors, published by Springer Nature. f) Coalescence of hollow vesicle-like droplets from RNA-protein complexes. Scale bars = 10  $\mu\text{m}$ . Reproduced with permission.<sup>[82]</sup> Copyright 2020, National Academy of Sciences. g) Multiphase LLPS resulting in “hollow” condensates. Scale bar = 20  $\mu\text{m}$ . Reproduced with permission.<sup>[84]</sup> Copyright 2021, Royal Society of Chemistry.

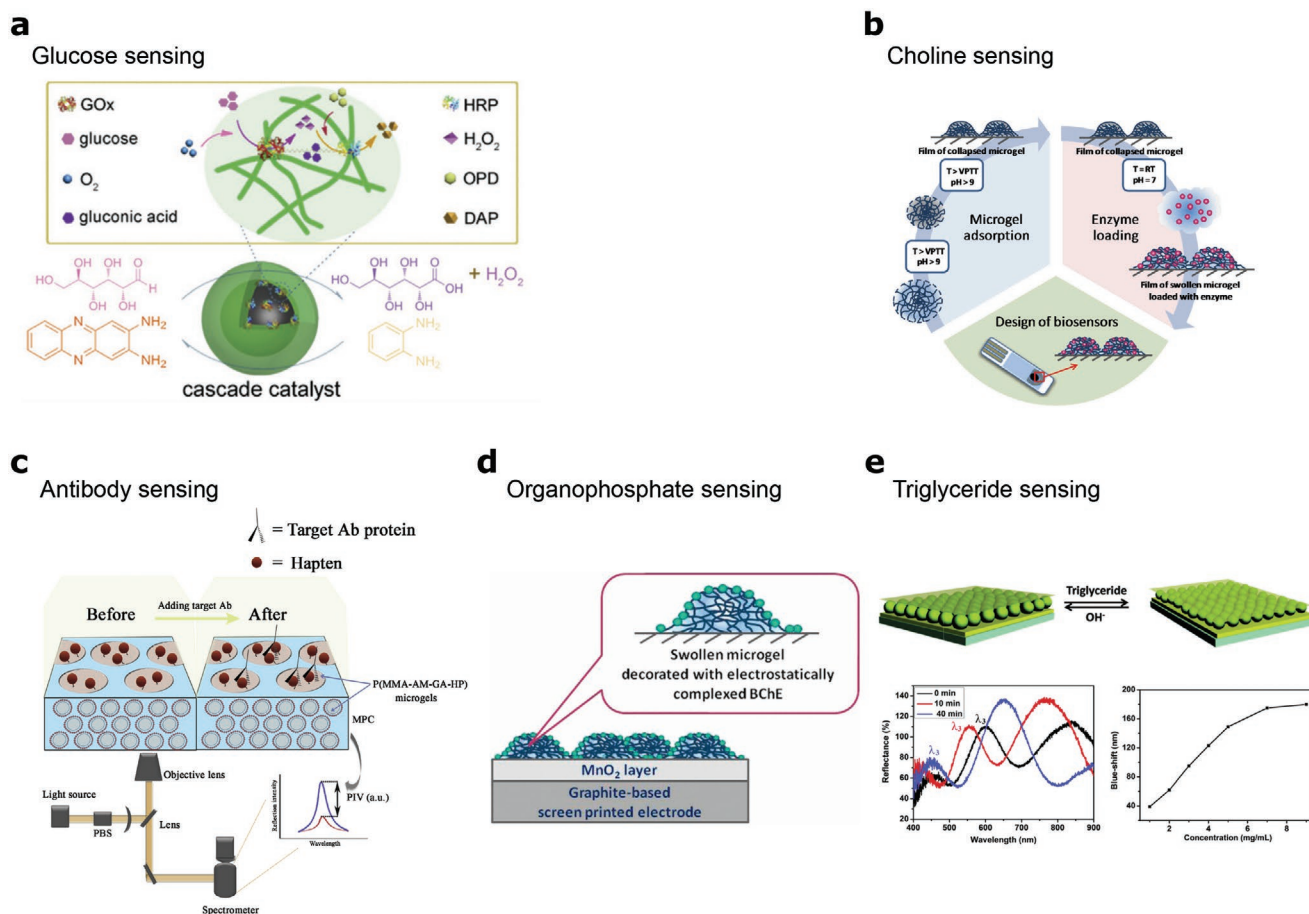


**Figure 4.** Microgels as miniaturized biosensors. a) Colorimetric detection of glucose through bienzyme-mediated free-radical polymerization. Reproduced with permission.<sup>[98]</sup> Copyright 2015, Royal Society of Chemistry. b) Sensing of choline with microgel/enzyme films. Reproduced under the terms of the Creative Commons CC BY license.<sup>[101]</sup> Copyright 2018, The Authors, published by MDPI. c) Antibody recognition with microgel photonic crystals. Reproduced with permission.<sup>[99]</sup> Copyright 2021, Elsevier. d) Sensing of organophosphorus pesticides with microgel approaches. Reproduced with permission.<sup>[100]</sup> Copyright 2017, American Chemical Society. e) Sensing of triglyceride with microgel-based optical devices. Reproduced with permission.<sup>[102]</sup> Copyright 2015, Royal Society of Chemistry.

undergone a secondary phase separation, creating distinct regions inside of the condensate.<sup>[80,81]</sup> Two immiscible liquids make up the condensate, and which phase is on outside or inside of the condensate depends on the relative surface tension values.<sup>[80,81]</sup> Additionally, the conditions leading to the demixing have been studied, particularly the role of nucleic acids, which are abundant in organelles in cells.<sup>[69,80,81]</sup> Studying multiphase condensates using microgels could offer further insight into this secondary phase separation. Size and surface tension can be readily controlled in microgels as well as phase transitions. This could be of interest to study the kinetics of a secondary phase transition. Additionally, a microgel system could be used to find what parameters influence the surface tension and thus the “order” of different phases, which in cells would influence the recruiting of molecules into the condensate and thus its function.

The second type of heterogeneity that has been observed is the formation of a polymer-poor phase inside of the condensates.<sup>[82,83]</sup> Vesicle-like droplets have been systematically studied to probe the phase behaviors of RNA-protein complexes (Figure 2f).<sup>[82]</sup> This phenomenon is being increasingly

investigated, making microgel models very valuable. Poly(*N*-isopropylacrylamide) (PNIPAM) microgels with xanthan polymer (a depletant) might be a suitable model system to study this behavior, as they have been observed to form core-shell-like structures through LLPS (Figure 2g).<sup>[84]</sup> At room temperature (RT), the dispersed phases are liquid; at elevated temperature, the dispersed particles gelate and aggregate, and form microgels with solid shells.<sup>[84]</sup> LLPS systems are achieved when cooling down again to RT, indicated by the coalescence of multiple inner droplets.<sup>[84]</sup> In different material systems, LLPS is achieved by decreasing to or increasing from RT.<sup>[4,8,84]</sup> Light-sheet microscopy can facilitate the study of LLPS with the colloid-polymer system subjected to shear, and it is possible to track the deformation of the liquid droplets as a function of shear rate.<sup>[85]</sup>

### 3. Micromechanics of Soft Microgels

A key characteristic of microgels influencing their applications in biomedical areas is their mechanical deformability and

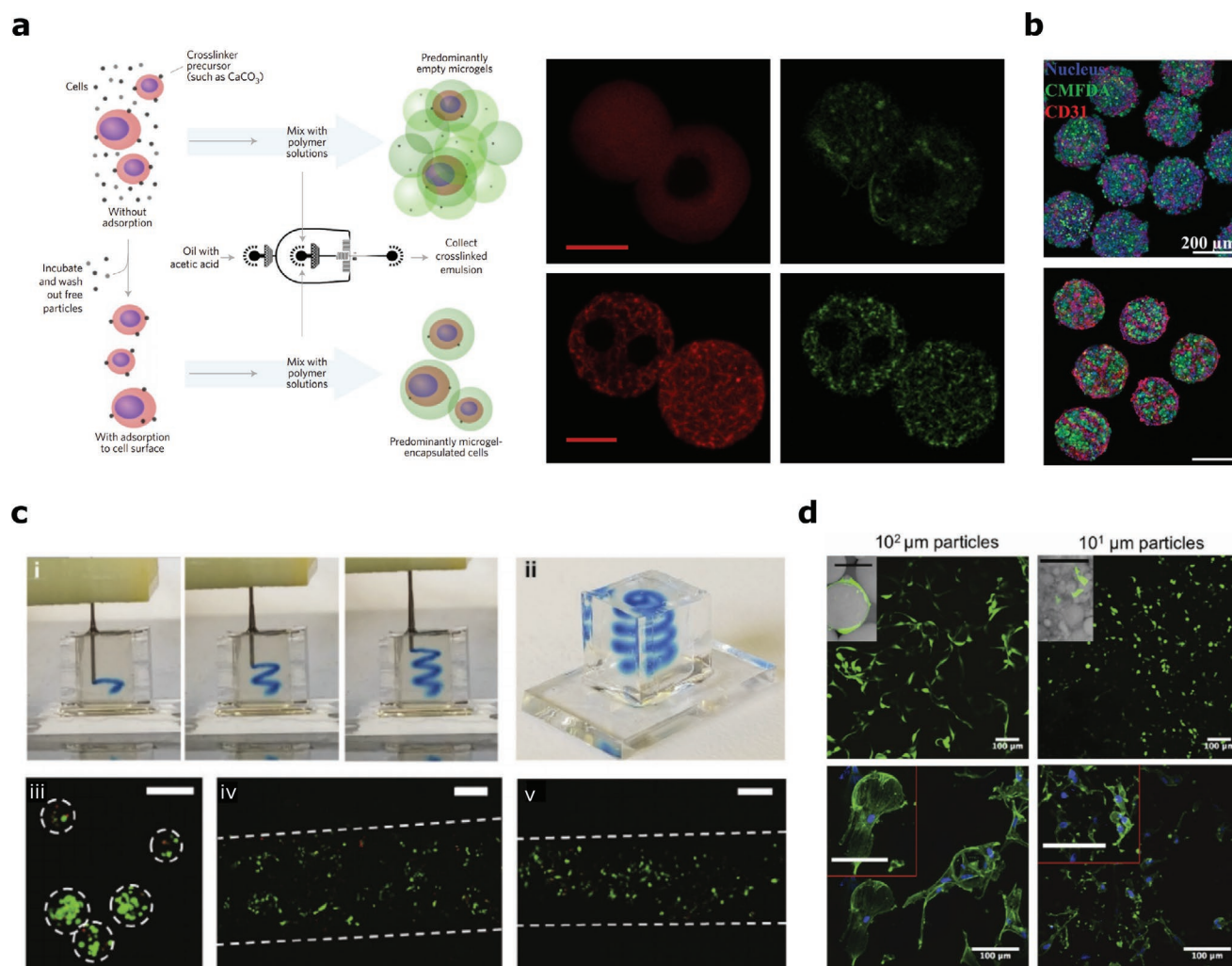


**Figure 5.** Applications of microgels in cell culture. a) Cell encapsulation in alginate microgels. Confocal images of alginate-collagen microgels (top right: green, collagen; red, alginate) and alginate-fibrin microgels (bottom right: green, fibrin; red, alginate). Scale bars = 20  $\mu\text{m}$ . Reproduced with permission.<sup>[2]</sup> Copyright 2017, Springer Nature. b) Biomimetic hepatic-lobule-like structures without (top) and with (bottom) compartments. Scale bar = 200  $\mu\text{m}$ . Adapted with permission.<sup>[34]</sup> Copyright 2021, WILEY-VCH. c) 3D printing ((i),(ii)) of microgel inks (with blue dye) in a spiral pattern into a shear-thinning support hydrogel (transparent). 3T3 fibroblasts encapsulated in microgels before ((iii)) or after 3D printing ((iv),(v)). Scale bars = 200  $\mu\text{m}$ . Reproduced under the terms of the Creative Commons CC BY license.<sup>[9]</sup> Copyright 2018, The Authors, published by WILEY-VCH. d) Human mesenchymal stem cells on the surfaces of microgels. Scale bars = 100  $\mu\text{m}$ . Adapted with permission.<sup>[122]</sup> Copyright 2017, WILEY-VCH.

elastic modulus. To probe the micromechanical properties of microgels, both glass-capillary microfluidics and polydimethylsiloxane (PDMS)-based microfluidics are used (Figure 3).<sup>[86,87]</sup> Determining the elastic properties of these soft and deformable materials is key, but probing them at the microscale has been challenging.<sup>[86]</sup> Though methods such as atomic force microscopy (AFM) and micropipette aspiration have been employed to monitor the mechanical response of materials at small scales, it is challenging to position the materials such as microgels under optical microscopes.<sup>[86,88,89]</sup> Besides, AFM and micropipette aspiration approaches are localized methods to probe the elasticity of soft materials or particles, not illustrating the deformation of an entire particle.<sup>[8,87]</sup> It would be advantageous to develop micromechanical methods to quantify the mechanical properties from the whole microgel.<sup>[87]</sup> Such methods of micromechanical measurement can save the

amount of samples, and can complement bulk methods such as rheology.<sup>[87]</sup>

A glass-capillary approach, termed capillary micromechanics, has been investigated to characterize the mechanical properties of microgels. Both the compressive and the shear moduli can be extracted from the stress-strain relationships (Figure 3a).<sup>[86,90]</sup> These results agree well with bulk studies. In brief, a single microgel is trapped in the tapering tip of a glass capillary coated with bovine serum albumin, and the deformation of the microgel under varying liquid pressure can be analyzed and reflect the elastic properties of the microgel.<sup>[86]</sup> However, only a single microgel can be explored each time, which can limit the efficiency and accuracy of the methods. Using this glass-capillary approach, the particle deforms in a capillary.<sup>[86]</sup> By contrast, using a micropipette aspiration method, a particle deforms between a capillary tip and a beam surface.<sup>[88]</sup>

**Table 1.** Materials commonly used for microgel/microfluidic studies.

Material	Cell lineage	Microfluidic technique	Gelation method	Applications, key findings or advances	Ref.
Alginate	Hepatocytes and fibroblasts	Core-shell spheroids based on microdroplet making techniques	Ca <sup>2+</sup> release from EDTA-Ca	3D core-shell scaffold is made. High-level liver-specific functions have been achieved with the coculture of hepatocytes and fibroblasts. It is potential for in vitro liver model for high-throughput drug screening assays.	[51]
	Murine marrow stromal cells (mMSCs), human MSCs, and K-562 chronic myelogenous leukemia cells	Spheroids based on microdroplet making techniques	Ca <sup>2+</sup> release from calcium nanoparticles	Alginate, alginate-collagen, alginate-fibrin microgels have been made with cells encapsulated. Increased osteogenesis is found in harder microgels than softer microgels in vivo. The donor cells have been protected from immune clearance in the microgels injected into mice.	[2]
	None	PDMS-based chips	Fusion of alginate droplets and Ca <sup>2+</sup> droplets	No extra chelators are used in the approach. Alginate droplets and Ca <sup>2+</sup> droplets fuse through a picoinjection strategy on chip. Spherical and nonspherical microgels can be produced under various picoinjection conditions.	[233]
Collagen	Breast cancer cells, endothelial cells, and human umbilical vein endothelial cells (HUVECs)	Cell culture on chip	pH induced gelation of collagen	A 3D circular microvessel of about 100 µm in diameter has been formed with extracellular in a microfluidic device. Endothelial layers have reduced the cancer exit events over the culture period. Single-cell behavior can be easily analyzed in the micro channels in 3D.	[97]
	HEK 293 embryonic kidney cells; NIH 3T3 murine fibroblasts; MC 3T3 murine osteoblast precursors' cell line; MCF10A epithelial cells.	Collagen microgels from aqueous two-phase systems	pH induced gelation of collagen	Aqueous two-phase systems (PEG and dextran) have been used to template collagen microgels. Collagen droplet contraction rates depend on cell density and the presence of growth factors. The diffusion of growth factors in collagen microgels is faster than that in the conventional collagen assay.	[234]
Agarose	Endothelial cells, and HepG2 cells	Cell culture on hydrogel-based device	Cooling to gelate agarose, pH induced gelation of collagen	A natural leaf has been used as mold to make agarose-based microfluidic devices, and collagen has been filled in the channels of the devices. The addition of collagen in the microfluidic channels have slowed down the perfusion of small molecules. Vascularized cancer tissues have been made and studied dynamically with increased spreading of endothelial cells.	[235]
	Adenoid cystic carcinoma cells	Droplet making and trapping on-chip	Cooling to gelate agarose	Two-layer PDMS devices have been fabricated for microgel trapping. Carcinoma cells have been encapsulated in the microgels for tissue engineering studies.	[206]
Gelatin methacrylate (GelMA)	HUVECs and fibroblasts	Cell culture on and in GelMA-based micro environments	Photo-cross-linking of hydrogel with UV and photo-initiator	Cell adhesion to 2D GelMA surfaces has shown that variation of stiffness of GelMA hydrogels is associated with cell morphology and confluency. Cell growth in 3D GelMA micro patterns has shown that the increasing of hydrogel stiffness leads to the increase of cell confluency. Perfusable microvasculature and endothelial linings have been created in the microfluidic channels.	[184]
	Bone marrow-derived mesenchymal stem cells (BMSCs)	Microgel generation with capillary microfluidic devices	Photo-cross-linking of hydrogel with UV and photo-initiator	Cells and growth factors are encapsulated in the GelMA microgels. Significant osteogenesis has been displayed by relevant protein and mineral in the 3D in vitro culture of BMSCs. The cells with growth factor in the microgels have increased performance of in vivo bone formation.	[189]

Table 1. Continued.

Material	Cell lineage	Microfluidic technique	Gelation method	Applications, key findings or advances	Ref.
Gelatin	None	Microgel generation with PDMS-based microfluidic devices	Physical and/or enzymatic cross-linking	Protein microgels with varying radial density have been fabricated through versatile cross-linking and controlled microfluidic mixing. Protein microgels can act as the precursors of all-aqueous LLPS (two-phase). Core-shell microgels can be the outcomes and the precursors of all-aqueous LLPS (multiphase).	[3,4,8]
Amyloid proteins	None	Microgel generation with PDMS-based microfluidic devices	Self-assembly of nanofibrils	Amyloidogenic protein Ure2 has been used as a self-assembling material for microgel formation. Microfluidics enables the formation of monodisperse droplets with controlled amount of protein trapping. Multiphase microgels with lysozymes demonstrate a high-throughput platform for controlling aggregation and structuring of fibrillar proteins.	[53,216]
DNA hydrogel	None	Microgel generation with PDMS-based microfluidic devices	Chemically cross-linked or physically entangled DNA	A DNA microgel platform (cell-free) for protein production that plans for a phenotype-genotype connection has been developed with DNA microgels. Fluorescent cell sorting of the microgels can be used to enrich gene concentration, in the context of gene isolation and protein display. DNA microgels can be applied to biosensing, drug delivery, and gene therapy.	[228,229]

A PDMS-based approach has been reported to carry out the mechanical testing of multiple solid microgels in parallel, increasing the efficiency of testing (Figure 3b,c).<sup>[87]</sup> It is also possible to average the elastic moduli of the microgels to achieve higher accuracy. This PDMS-based microfluidic device, coated with polyethylene glycol (PEG), has multiple tapering channels in parallel and two bypass-flow channels. It is feasible to achieve 100% trapping efficiency in practice.<sup>[87]</sup> The analysis of the stress-strain relationships of the PDMS-based approach is similar to that of the glass-capillary approach.<sup>[86,87]</sup> Notably, the interfacial tension between the microgels and the aqueous continuous phase can be ignored,<sup>[87]</sup> and the situation would be different using an oil continuous phase.

In another study, the abovementioned PDMS-based device has been used to permanently buckle core-shell microgels (Figure 3b,d).<sup>[8,87]</sup> For this application, the continuous phase is oil.<sup>[8]</sup> The trapped core-shell microgels underwent several cycles of increase and decrease of the pressure of the oil continuous phase; water is squeezed out from the cores and then migrated to the space between the oil and the shell.<sup>[8]</sup> The flat surfaces of the PDMS walls also contribute to the buckling to relocate the excessive materials. Such buckling is similar to the buckling of a tennis ball with a smooth invagination.<sup>[8,91]</sup> The characterization of the elastic moduli of core-shell microgels from the stress-strain relationships might be complicated, in view of the buckling during the squashing (Figure 3d).<sup>[8,90]</sup> However, this device (Figure 3b) could offer a new route to deform especially buckle microgels, which could complement other factors such as osmotic pressure or interfacial tension.<sup>[8]</sup>

The mechanical property of microgels is usually inherited from that of bulk materials. The mechanical performance of relatively “big” microgels (for example, diameter > 20  $\mu\text{m}$ ) can be explored using microfluidic channels (Figure 3a–d).<sup>[8,86,87]</sup> The mechanical property of “big” microgels may be different

from “small” microgels because of size effect. For “small” microgels (for example, diameter  $\approx$  300 nm) that do not easily match the size of microfluidic channels, AFM with fine tips can be a promising tool to probe their mechanics in liquid environment.<sup>[22]</sup>

The mechanical property especially the elasticity of materials can have varying implications on functional roles of the microgels. For example, silicone, skin, soy protein, whey protein, synthetic polymers, amyloid fibrils, and silk have demonstrated increasing and somewhat overlapping stiffness, and the stiffness-strength maps of a range of materials can guide the selection of materials for specific engineering purposes.<sup>[92,93]</sup> Designing microgels for industries would benefit from the consideration of the mechanical properties of materials. For example, the degradable microbeads in shampoo or liquid soap are expected to demonstrate corresponding stiffness for better user experience. In terms of biological relevance, the stiffness of tissues or organs also varies significantly.<sup>[94]</sup> For example, brain and lung are soft organs, while muscle tissues have intermediate stiffness.<sup>[94]</sup> Cartilages and bones have high stiffness, as they are exposed to high mechanical loading in vivo.<sup>[94]</sup> The optimization of the mechanical property of the microgels or hydrogels for tissue engineering would contribute to the generation of more biomimetic cellular structures. One of the major components of vascular vessel walls is collagen, and collagen microgels or channels have been developed as injectable or on-chip angiogenic 3D constructs.<sup>[95–97]</sup>

#### 4. Microgels as Biosensors

Microgels offer a biomimetic environment within which enzymes and other active components can be localized. As such, microgels have emerged as promising materials for the

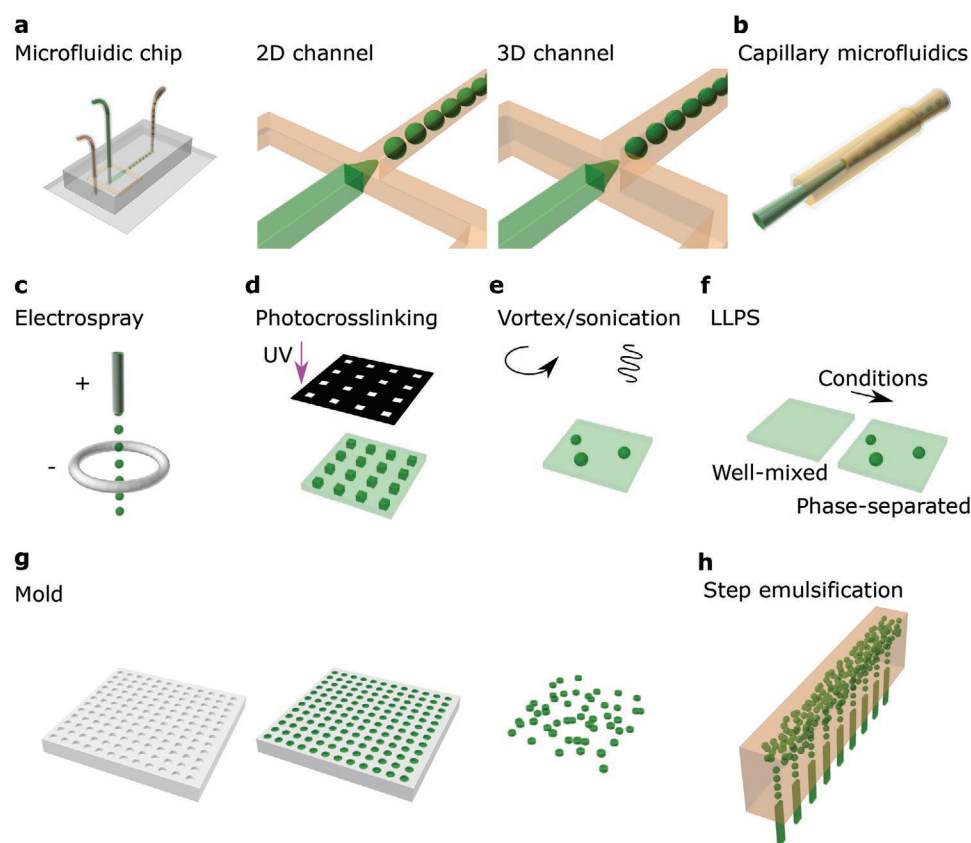


**Figure 6.** Microgel fabrication methods. The methods can include a) 2D microfluidic chips,<sup>[3,8]</sup> 3D microfluidic chips,<sup>[237]</sup> Reproduced under the terms of the Creative Commons CC BY license.<sup>[3]</sup> Copyright 2020, The Authors, published by WILEY-VCH; Reproduced under the terms of the Creative Commons CC BY license.<sup>[8]</sup> Copyright 2021, The Authors, published by WILEY-VCH; Reproduced with permission.<sup>[237]</sup> Copyright 2012, American Institute of Physics. b) capillary microfluidics,<sup>[267]</sup> Reproduced with permission.<sup>[267]</sup> Copyright 2007, WILEY-VCH. c) electrospray,<sup>[241]</sup> Reproduced with permission.<sup>[241]</sup> Copyright 2015, American Chemical Society. d) photo-cross-linking. Reproduced with permission.<sup>[340]</sup> Copyright 2018, WILEY-VCH. e) Vortex and/or sonication. Reproduced with permission.<sup>[122]</sup> Copyright 2017, WILEY-VCH. f) LLPS in vitro,<sup>[59]</sup> Reproduced with permission.<sup>[59]</sup> Copyright 2020, Springer Nature. g) molds,<sup>[248]</sup> Reproduced with permission.<sup>[248]</sup> Copyright 2012, American Chemical Society. and h) step emulsification.<sup>[252]</sup> Reproduced with permission.<sup>[252]</sup> Copyright 2018, Royal Society of Chemistry.

sensing of biomolecules (Figure 4).<sup>[98–104]</sup> Microgels can be used for the sensing of glucose, RNA/DNA, enzymes, antibodies and even physical cues. The advantage of using microgels over conventional sensors is that they maintain a hydrated and non-denaturing environment to protect the bioactive components required for detection.<sup>[98–102]</sup> Most of the current microgel

biosensors are used in vitro, with the aim of applying them for in vivo measurements in the future.<sup>[105,106]</sup> In terms of medical diagnostics and personalized medicine, microgels are also a promising and sensitive tool. For example, a droplet-trapping assay can be used with hydrogel microspheres for the highly sensitive detection of vascular endothelial growth factor.<sup>[107]</sup> Hydrogels with tunable porosity improved mass transport, and this method demonstrated higher efficiency compared with ELISA, Luminex assays, and previous studies.<sup>[107]</sup> Furthermore, it has been reported that microarray analysis can be combined with nucleic acid sequence-based amplification with self-reporting molecular beacon probes that fluoresce upon hybridization for real-time microbial molecular diagnostics.<sup>[108]</sup>

**Table 2.** Commonly used oils and surfactants for microdroplets or microgels.

Oil	Surfactant	Ref.
Mineral oil	Span 80/Tween 80/ABIL/Triton X-100	[5,282]
Fluorinert FC-40	PEG-PFPE surfactant	[3,4,8,27]
HFE-7500	PEG-PFPE surfactant	[2,287]
Silicon(e) oil	DC547/Span 80	[295,296]
Oleic acid	Span 80 or none	[293,297]
Hydrocarbon and silicone oil	Lipid	[183,298]
N-octane	None	[292]

#### 4.1. Glucose Sensing

For glucose sensing by a colorimetric method (Figure 4a), glucose oxidase and horseradish peroxidase are loaded in core-shell microgels.<sup>[98]</sup> A glucose dose-response curve could guide the application of the microgels in glucose testing, and the

**Table 3.** Several demulsification examples.

Demulsification approach	Oil	Surfactant	Microgel material	Ref.
Perfluoro demulsifiers and centrifugal force	Fluorinert FC-40	PEG-PFPE surfactant	Alginate and gelatin	[2,3]
HCl and centrifugal force	Fluorinert FC-40	PEG-PFPE surfactant	Lysozyme fibrils	[220]
Pluronic F-127 and centrifugal force	Mineral oil	Span 80	Hydrogels modified by matrix metalloprotease-sensitive peptides	[127]
Antistatic gun	Hydrofluoroether (HFE)	PEG-PFPE surfactant	Only qPCR mix liquid, no hydrogels	[299]
Repetitive replacement of the continuous phase	Hydrocarbon and silicone oil	Lipid	Matrigel and collagen	[183,298]

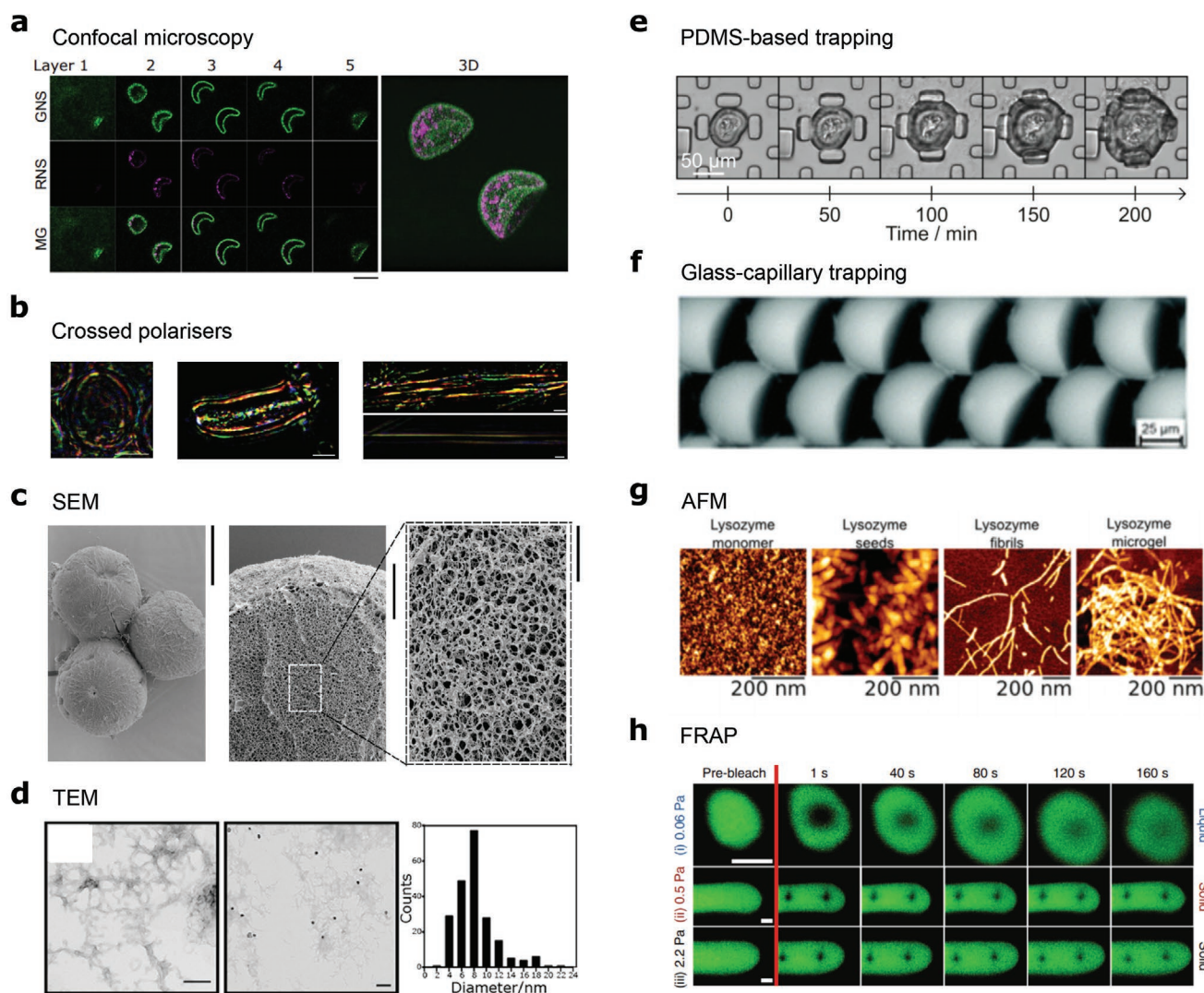


**Figure 7.** Several characterization methods commonly used for the understanding of microgels. a) 3D reconstruction of confocal imaging of buckled core-shell microcapsules. Scale bar = 100  $\mu$ m. Reproduced under the terms of the Creative Commons CC BY license.<sup>[8]</sup> Copyright 2021, The Authors, published by WILEY-VCH. b) Optical microscopy imaging with crossed polarizers to understand silk micrococoon structures. Scale bars = 10  $\mu$ m. Reproduced under the terms of the Creative Commons CC BY license.<sup>[1]</sup> Copyright 2017, The Authors, published by Springer Nature. c) SEM imaging of gelatin microgels. Scale bars = 40  $\mu$ m (left), 10  $\mu$ m (middle), and 2  $\mu$ m (right). Reproduced under the terms of the Creative Commons CC BY license.<sup>[3]</sup> Copyright 2020, The Authors, published by WILEY-VCH. d) TEM imaging of silk nanofibrils without (left) and with silver nanoparticles (middle) and the size distribution of the silver nanoparticles (right). Scale bars = 200 nm. Reproduced with permission.<sup>[301]</sup> Copyright 2020, American Chemical Society. e) Trapping of microgels in a PDMS-based chip. Scale bar = 50  $\mu$ m. Reproduced with permission.<sup>[120]</sup> Copyright 2015, National Academy of Sciences. f) Trapping of microgels in a glass capillary. Scale bar = 25  $\mu$ m. Reproduced with permission.<sup>[311]</sup> Copyright 2016, Royal Society of Chemistry. g) AFM imaging of lysozyme monomers, seeds, fibrils, and microgel. Scale bar = 200 nm. Reproduced with permission.<sup>[220]</sup> Copyright 2015, American Chemical Society. h) Time-lapsed imaging for FRAP analysis. Scale bars = 1  $\mu$ m. Reproduced with permission.<sup>[59]</sup> Copyright 2020, Springer Nature.

**Table 4.** Several characterization skills for the understanding of materials or microgels.

Characterization skill	Purpose	More details	Ref.
Optical microscopy	Morphology, crystal structure, degradation, molecule location and drug release, conformation	Static or time-lapsed, crossed polarizers, 2D or 3D, confocal imaging	[1,3,4,8,52]
Electron microscopy (SEM or TEM)	Morphology, porosity, fibrillar structure	TEM, SEM, or cryo-SEM, EDS mapping	[3,300,301]
Transmission X-Ray Microscopy	Morphology, microgel arrangement, thermoresponsive behavior	Tomographic imaging of microgel-covered droplets, 3D reconstruction	[302,303,315]
X-Ray scattering (SAXS or WAXS) and neutron scattering (SANS)	Crystallinity, network formation, size information	Static or time-resolved	[304,305,309]
Microfluidic chip	Mechanical testing, trapping, deformation (buckling)	Multiple microgels	[8,87,120,316]
Glass capillary	Mechanical testing, trapping	Single microgel for mechanical testing, multiple microgels for trapping	[86,217,311]
Spectroscopy (CD, fluorescence, FITR, IR)	Conformation changes, kinetics, secondary structures, hydrogen bonding	Microgels, bulk materials, static or time-lapsed	[1,59,220,262]
AFM	Morphology, mechanical testing	Nanofibrils, microgels	[22–24,89,216,220,317]
FRAP	Solid or gel phase determination, diffusion coefficient	Mobility of molecules or particles in gels or in liquids, LLPS characterization, phase determination	[59,318,319]
Cell culture	Biocompatibility of materials	In vivo or in vitro, cell encapsulation, cell adherence	[2,16,28,320]
SRFM	Imaging of “small” microgels (nanometer or submicron)	Visualization of cross-linker positions; capturing microgel geometries under dilute or densely packed conditions.	[18–21]

method is selective for glucose among several saccharides.<sup>[98]</sup> Thermosensitive and electroactive microgel particles are also fabricated for glucose testing, and the sensors work satisfactorily at a temperature close to the human body temperature.<sup>[109]</sup> The microgels functionalized with amino-ferrocene and glucose oxidase are stable for 3 months after their synthesis.<sup>[109]</sup>

## 4.2. DNA and/or RNA Sensing

Microgel probes for the fluorescence detection of nucleic acids have been applied to detect genetic materials of viral pathogens such as HIV and HCV and SARS.<sup>[110–112]</sup> Microgel-based devices could alter their optical properties in the presence of single-stranded DNA, as negatively charged DNA can result in the cross-linking and collapse of the positively charged microgels in the device.<sup>[113]</sup> Microgels can also contribute to the separation of RNA from DNA-RNA mixtures.<sup>[114]</sup> These miniaturized microgel platforms have a high potential to detect low abundant nucleic acids without amplification techniques.<sup>[110,113]</sup>

## 4.3. Enzymes in Microgel Sensors

Temperature- and pH-sensitive microgels are complexed with the enzymes to detect the compound which the enzymes can bind to with high specificity.<sup>[98,101,109,115–117]</sup> For example, microgels with choline oxidase can be used to detect choline (Figure 4b).<sup>[101]</sup> Microgels are also able to measure the amount of a specific enzyme. The concentration of proteinase K can be quantified using the fluorescent intensity, which can also be used as an indication of the enzyme degradation rate.<sup>[115]</sup> A similar setup is used for sensing tyrosinase.<sup>[116]</sup> In cases

where low concentrations need to be detected, microgels can aid conventional immunodiagnostic assay by amplifying the signal.<sup>[118]</sup>

## 4.4. Sensing of Other Chemical Cues

The sensing of antibody proteins can be achieved by microgel photonic crystals (Figure 4c).<sup>[99]</sup> Tracing target antibody proteins is therefore possible without the use of label techniques, showing potential for medical diagnostics.<sup>[99]</sup> Organophosphorus compounds could be detected by microgels/butyrylcholinesterase biosensors (Figure 4d).<sup>[100]</sup> Such amperometric biosensors demonstrated long-term stability.<sup>[100]</sup> Triglyceride sensors show responsiveness to the concentrations of a triglyceride, and the sensors are fabricated by coating microgels onto gold layers (Figure 4e).<sup>[102]</sup> Similarly, estradiol-17 $\beta$  biosensors are used to detect estradiol-17 $\beta$  in aqueous solutions and milk samples by monitoring the reflectance peak shifts.<sup>[119]</sup>

## 4.5. Sensing of Physical Cues

Microgels could also function as sensors of temperature and stress.<sup>[4,8,87,120]</sup> For example, due to elevated temperature, the microgels described in Section 2 which undergo a gel–sol transition can demonstrate shape changes in aqueous surroundings (Figure 2a–c).<sup>[4,8]</sup> The deformation of cantilevers can determine the force generated during amyloid growth (Figure 7e).<sup>[120]</sup> Wearable devices and electronic skins made from microgels have been developed, which are responsive to pressure changes to enable the monitoring of cardiovascular risk factors.<sup>[121]</sup>

## 5. Cell-Culture Scaffolds

An important area of application of microgels is in developing next generation biomimetic and 3D cell culture environments and scaffolds both *in vitro* or *in vivo* (Figure 5 and Table 1).<sup>[2,5,122–127]</sup> Hydrogels are particularly suitable as substrates for 3D cell culture because they resemble in terms of their mechanical properties the native extracellular matrix (ECM) and have tunable biochemical and biophysical properties.<sup>[128–130]</sup> Unlike monolayer-based cell culture, hydrogels create an environment where cells can attach, grow, proliferate, migrate, and communicate with the ECM in 3D,<sup>[131]</sup> thus bridging the gap between 2D and physiological scenarios. Hydrogels have allowed cell biology research to utilize the third dimension. Meanwhile, increasing efforts are being made to use microgels, rather than the macroscaled hydrogels, because microgels have some unique advantages for this purpose. First, the scale-down size gives rise to a higher surface-to-volume ratio and shorter diffusion lengths,<sup>[132]</sup> facilitating the efficient delivery of nutrients and oxygen to the cells. Second, due to the discrete nature of microgels, multifunctional composite microgels can be generated by facilely mixing different microgel populations carrying distinct functions<sup>[133,134]</sup> or by microfluidic programming.<sup>[135]</sup> Third, the micron-level size and the collective shear-thinning behavior of granular microgels enable injection through needles and tubings, which is particularly favorable in cell delivery, tissue engineering, and bio-ink technology.<sup>[2,5,126,127,129,136]</sup> Last, high-throughput fabrication of cell-laden microgels and *in situ* cell growth monitoring and characterization can be achieved.<sup>[137,138]</sup>

In the context of microgel-based 3D cell culture, one way is to place cells as near the microgel geometrical center as possible to prevent anisometric stimulations and cell escaping during long-term cell culture. However, off-center cell positions are constantly observed using traditional homogeneous microgels.<sup>[139,140]</sup> 3D microfluidic chips or glass capillaries are promising tools to locate cells in the center of the microgels. A one-step 2D method has been reported to generate core-shell microgels with an aqueous core and a photo-cross-linkable gelatin methacryloyl (GelMA) shell and recently a more complex microgel morphology of multi-aqueous cores.<sup>[141,142]</sup> Cell-secreted proteinases during matrix remodeling also contribute to cell egressing.<sup>[140]</sup> A stepwise encapsulation approach is employed to enclose the cell-laden biodegradable microgel in a nondegradable microgel.<sup>[143]</sup> In this way, cells are preserved inside for long-term cell culture, and biophysical cues such as matrix stiffness can be easily tuned. By providing a protective layer for cells encapsulated, inhomogeneous microgels have paved a new way of cell assembly. A water/water/oil double emulsion pipeline for generating core-shell microgels has been reported;<sup>[51]</sup> in this work, HepG2 cells are encapsulated in the aqueous core while NIH-3T3 cells in the alginate shell, thereby homotypic and heterotypic cell interactions could be established spatially at the same time, which is challenging to achieve using conventional 2D cell culture techniques. Double emulsion technique can also assist in microgel fabrication process in terms of bypassing the use of carrier oil in droplet microfluidic settings. Inhomogeneous microgels comprising GelMA hydrogels are coated with an ultrathin oil layer as the middle phase;<sup>[144]</sup> the oil

phase dewets immediately upon the gelation of GelMA, giving rise to an all-aqueous environment for microgel fabrication. In a recent study, a precursor cartridge and microfluidic emulsification are combined for the generation of nonstructured (noncompartmentalized) and structured (compartmentalized) collagen microgels (Figure 5b);<sup>[34]</sup> homogeneous and inhomogeneous mini liver models have been correspondingly developed, and demonstrate remarkable differences in protein synthesis, drug metabolism, and transplant performance.<sup>[34]</sup>

## 6. Other Promising Applications

### 6.1. Gene Delivery

Molecular medicine is undergoing a transformation with the advent of new modalities including iRNAs and enzymes such as CRISPR.<sup>[145,146]</sup> These modalities allow the targeting of previously undruggable systems; however, a central challenge is the delivery of these species to the target tissues. Great progress has been demonstrated with lipid nanoparticles, but challenges remain, in particular with delivery into tissues outside of the liver, and long term sustained release of actives. Polymers in the forms of hydrogels can function as the carriers of nucleic acids to cells or tissues for gene therapies, in addition to other nonviral vectors such as nanoparticles or lipids.<sup>[147–149]</sup> Through the new nonviral protocols, a variety of nucleic acids can be delivered to targeted sites for the precaution and treatment of diseases.<sup>[147,148]</sup> A layer-by-layer microgel system has been developed for 3D cell culture and localized gene delivery by postloading nonviral vectors.<sup>[150]</sup> The surfaces of microgels could be modified to influence the DNA adsorption-desorption outcomes;<sup>[151]</sup> for example, microgels with polycationic brushes could increase the DNA adsorption, and the DNA can be desorbed by tuning pH.<sup>[151]</sup> Degradable and small microgels with a cationic pH-temperature sensitive core and a hydrophilic shell are developed for gene delivery, and have demonstrated effective release of nucleic acids into cancer cells.<sup>[152]</sup> The release of siRNA has been exploited from microencapsulated nanogels (small microgels) for the treatment of inflammatory bowel diseases;<sup>[153]</sup> the gene carriers are designed to be protected in acidic stomach environment and then enzymatically degraded in intestinal regions, and thus have potential for oral medicine.<sup>[153]</sup> Microgels with antisense oligonucleotides have been injected *in vivo*, showing sustained gene delivery for the treatment of Duchenne muscular dystrophy.<sup>[154]</sup>

### 6.2. Additive Manufacturing

Microgel-laden bio-inks have been used in 3D printing (additive manufacturing).<sup>[129,155]</sup> A cell-friendly all-aqueous material system consisting of PEG and GelMA is used as 3D porous cell-culture scaffolds.<sup>[155]</sup> Jammed-microgel 3D printing has also been reported,<sup>[5,156]</sup> and rheology characterizations on viscosity, shearing-yielding, and shear-thinning are conducted; these microgels could be printed either on the surfaces or within

the hydrogels.<sup>[5]</sup> Freeform reversible embedding of suspended hydrogels is also used for the printing of cell-laden oxidized methacrylated alginate microgels, and femur, skull, and ear models are separately fabricated.<sup>[129]</sup>

### 6.3. Cosmetics

Microgels have also been used in cosmetics. For example, oligo(ethylene glycol)-based microgel dispersions are used to form transparent films, which encapsulate different types of UVA and UVB-absorbing molecules.<sup>[157]</sup> Interestingly, microgels have the ability to release compounds at different rates based on the compound hydrophobicity. The transitional phase inversion behavior of fumed silica–perfume oil–water emulsions is reported, which shows an example for perfume research and applications and opens up the possibility of perfume encapsulation in microgels for long-term storage or controlled release.<sup>[158]</sup>

### 6.4. Robots

Microgels could also function as the building blocks of robots composed of both soft and rigid microstructures.<sup>[159,160]</sup> Soft-robotics is a relatively new research field, focusing on designing robots that can easily interact with humans and delicate materials or objects. Microgels are specifically suitable for these robots since they can have a range of physical parameters. A micro robot based on tunable structures is developed and controlled by magnetic fields.<sup>[159]</sup> L-shaped hydrogels, spherical hydrogels, triangle hydrogels, and hexagonal hydrogels have demonstrated the potential of being assembled in multiple layers in versatile geometrical manners.<sup>[159]</sup> This can be used to measure or respond to bioactive molecules and other environmental stimuli on tissue growth or cellular processes.<sup>[159]</sup> Deformable core–shell microcapsules could also be used for the joints of soft robots based on their responsiveness to interfacial tension, osmosis, and mechanical pressure.<sup>[8]</sup>

### 6.5. Food

Microgels are increasingly used in the food industry.<sup>[56,161]</sup> Long-term stable submicron particles from food-grade whey protein are developed, and microgels in oil or aqueous phase could be used for the delivery of oil-soluble or water-soluble nutrients.<sup>[162]</sup> Emulsions stabilized by small particles, known as Pickering emulsions, are especially desirable for the food industry,<sup>[163]</sup> since they could serve as an alternative to conventional surfactants which can cause adverse effects such as irritation and hemolysis.<sup>[163]</sup>

## 7. Diversity in Materials for Microgels

Hydrogels and their composites have micro- or macroscopic spatial network structures, and aqueous solutions fill in the spaces in between for scaffolding, barriers, cell encapsulation, and drug delivery carriers.<sup>[164]</sup> Applications include the *in vivo*

or *in vitro* repair of bones, cartilages, nerve systems, vascular vessels, skins, livers, kidneys, hearts, or their substitutes with natural hydrogels such as polysaccharides and polypeptides, as well as synthetic hydrogels such as poly(acrylic acid) and its derivatives.<sup>[165,166,189]</sup> Physically cross-linked gels are usually not stable in the long term, as the cross-linking requires static electricity, hydrogen bonds, or spatial entanglement, which when removed causes the gel to lose shape. Oppositely, chemically cross-linked gels are structurally more permanent, and thus more suitable for biological and physiochemical applications *in vivo* or *in vitro*.<sup>[167]</sup> Gels, particularly microgels, could also be morphologically versatile including columns, porous sponges, fibers, membranes, and spheroids or beads.<sup>[168]</sup> Hydrogels, either naturally derived or synthetic, could be sensitive to external stimuli, and biosensors and bioswitches have been tested for signal control and controlled release.<sup>[169–171]</sup>

Microgel particles can be synthesized using emulsion polymerization, anionic copolymerization, cross-linking of adjacent polymer chains, and inverse micro-emulsion polymerization.<sup>[172]</sup> This reduces batch differences of the microgels, which makes the microgel scaffolds for tissue growth suitable for medical purposes. Those standards for the microgels may be defined by the biomaterials used, the sizes and the purposes of the application, and mass production in the future may also highlight the improvement in the quality control and global product tracking. In the rest of this section, we will discuss some materials from which microgels can be made (Table 1) in combination with microfluidic techniques.

Alginate acid is a natural product with linear structure consisting of homopolymeric blocks for tissue engineering.<sup>[2,173]</sup> Alginate sodium is water-swallowable and could be cross-linked covalently or ionically to form hydrogels or sponge scaffolds, which are mainly used for controlled drug release and the biocompatible micro carriers for genes, proteins, or cells.<sup>[2,16,51,174]</sup> Alginate sodium has been used for tissue/organ engineering, specifically for the regeneration of skins, cartilages, livers, bones, and vascular vessels.<sup>[175]</sup> However, the poor mechanical strength may hinder its application in rapid prototyping, and may also lead to the lack of mechanical support for cells. Modifications can be considered in mechanical performances and specific biological functions such as intercellular communications and signal transduction. A large number of literature has investigated the gelation (chelation) of alginate at small scales, and divalent cations have been frequently used.<sup>[2,25,176]</sup> The divalent cations can be from the aqueous solution injected (on chip), from the oil injected (on chip), or from the bath that collects the microgels (off chip).<sup>[2,25,176]</sup>

Collagen and collagen-derived hydrogels (such as gelatin) are also ideal for ECM materials with proper porosity, biodegradable rate, permeability, and surface physiochemical properties.<sup>[3,161,177–180]</sup> Collagen hydrogels have triple helical structures, and could sustain and reinforce the tissue-engineered products with regulatable ECM circumstances.<sup>[174,179]</sup> The biomedical applications of collagen have indicated its potential in more complicated construction of biological structures as a result of its functions such as guiding and chemotaxis.<sup>[181]</sup> Adjusting the pH is a common method to gelate the collagen. Collagen at lower pH is in liquid form with flowability;<sup>[97]</sup> at elevated pH (e.g., neutral pH), collagen hydrogels would emerge.<sup>[97,182]</sup> In a

study, neutralized collagen microgel is further stabilized covalently by 4S-StarPEG, mimicking the physical and enzymatic cross-linking of collagen *in vivo*.<sup>[182]</sup> With flexible matrix, the system can foster possibilities for the optimization of stem cell microenvironment and the modeling of hind-limb ischemia model.<sup>[182]</sup> In another study, collagen microgels have been stacked to achieve macroscopic tubular structures in the context of the engineering of intestinal tissues.<sup>[183]</sup> The study demonstrates the construction of tubular tissues from intestinal organoids and protein scaffolds without additional chemical synthesis.<sup>[183]</sup>

GelMA is produced through the reaction of gelatin with methacrylic anhydride.<sup>[184–186]</sup> Owing to the functionality of methacryloyl groups, GelMA could undergo immediate UV-induced cross-linking.<sup>[185,187]</sup> There are thus potentials to adjust the physicochemical properties of GelMA.<sup>[187]</sup> Meanwhile, the Arg-Gly-Asp motifs and matrix metalloproteinase sites of GelMA could support relevant cellular behaviors.<sup>[188]</sup> For example, it has been reported that bone marrow-derived mesenchymal stem cells could be encapsulated into GelMA microgels to form the injectable osteogenic tissue constructs, which shows enhanced osteogenesis in animal studies, associated with a significant increase in mineralization.<sup>[189]</sup> Bio-inks from GelMA microgels can be further printed or assembled into larger-scale structures.<sup>[190–192]</sup> Combined use of gelatin and GelMA is promising for the development of microgel-based materials to form constructs with voids, as gelatin can be sacrificed while GelMA are more thermostable.<sup>[193]</sup>

Fibrins are fibrous proteins that are formed by the polymerization of thrombin and fibrinogen; the fibrin-based materials have shown the prospects in developing new cell/tissue culture systems for uniform cell distribution and rapid tissue grafts with less inflammatory reaction *in vivo*.<sup>[2,194–197]</sup> New technologies such as biomedical imaging, micro extrusion, inkjet printing, and magnetically induced cell assembly would also optimize the formation of the fibrin-based structures.<sup>[165,198–203]</sup> Multiple cross-linking regimes can be explored to improve the stability of fibrin microgels and their production efficiency. There are relatively few historical studies in the area of fibrin microgels. However, fibrin fibers demonstrate the largest extensibility of all protein fibers, which could open up new possibilities of the development of flexible constructs that can tolerate large deformation.<sup>[204]</sup> In one study, PNIPAM microgels are mixed with fibrin hydrogels to explore strain-dependent viscoelasticity, and a small amount of local stretch of fibrin can cause significant stiffening of the material system.<sup>[205]</sup>

Agarose can be cross-linked with decreasing temperature, with the phase-transition temperatures depending on different derivatives.<sup>[206,207]</sup> It has been widely used in electrophoresis, protein purification and immunodiffusion, bacterial culture, and 3D culture of human and animal cells.<sup>[208–210]</sup> As a result of the biocompatibility, potential to be modified, reversible thermo-induced gelation, and tunable mechanical properties, agarose is a promising material for the development of microgels.<sup>[211]</sup> In addition, its bio-inert nature avoids undesired absorptivity to proteins or cells, while its porous structure ensures molecule transport.<sup>[212,213]</sup> The bio-inert property can be coupled with microgel-based technologies. For example, agarose microgel culture could amplify single cells into an isogenic colony; this

provides ample RNA for deep sequencing of the colony and reduces error due to noisy single cell gene expression profiles.<sup>[214]</sup> Furthermore, it has been reported that agarose microgels with xenogeneic hamster islets could serve as bio-artificial pancreas in streptozotocin-induced diabetic mice.<sup>[215]</sup>

Amyloidogenic proteins, such as lysozyme and silk, have also been reported in the contexts of microgels or microfluidics.<sup>[53,216–219]</sup> Nanofibrils from amyloid proteins are initially thought to be related to the onset and development of diseases, and recent studies have demonstrated that these proteins or nanofibrils could be applied to the rational design of biomaterials, such as active catalytic scaffolds, bacterial coatings, and advanced “plastic” bags or microparticles.<sup>[56,92,220–223]</sup> In one study, the loading capacity and the release kinetics of silk microgels have been explored;<sup>[1]</sup> release profiles of antibody domains can be modulated by microgel morphologies under varying microfluidic conditions.<sup>[1]</sup> As an example of nature-inspired materials, amyloid materials can be assembled at different length scales, and usually beta sheets can be combined into more complicated hierarchical structures.<sup>[55,56,224,225]</sup> Recently, studies have shown that LLPS droplets can be the early stage of the formation of amyloid materials, proposing an elucidation of the emergence and growth of amyloid materials.<sup>[59,226,227]</sup>

DNA microgel is a promising form of microgels, which could be further applied to artificial cells in the field of synthetic biology.<sup>[228]</sup> Cell-free platforms have been developed for gene expression, for example, protein expression and display; the microgels from chemically or physically networked matrices that demonstrate different physical and genetic characteristics.<sup>[228]</sup> Functionalized DNA can be applied to responsive hydrogels or microgels for a range of biomedical applications, such as biosensing, drug delivery, and regenerative medicine.<sup>[229–232]</sup>

## 8. Fabrication Methods of Microgels

This section will describe the different fabrication methods of producing microgels. Tremendous progress has been made in making microgels using engineering approaches or concepts.<sup>[1,2,14]</sup> Microfluidic chips, glass capillaries, and some of the other methods used for microgel synthesis will be discussed (Figure 6).

### 8.1. Microfluidic Chips

A wide range of microgels are synthesized using droplet microfluidic platforms through the manipulation of gel-precursor solutions. Droplet microfluidics provides temporal, spatial, and chemical control of the microgel fabrication process through the ability to control local temperatures, surface tension, pH, mixing of contents, and exposure to external fields like electromagnetic radiation or voltage.<sup>[233–235,237,253,254]</sup> While microfluidic methods enable precise control of reagent concentrations, it is critical to identify stable operating conditions for reproducible microdroplet production.<sup>[65,255]</sup> The most commonly used microfluidic devices for heterogeneous microgels

are fabricated using conventional photo- and soft-lithography methods, although concentric glass capillary devices are also used.<sup>[216,256,257]</sup>

Microdroplet generation approaches include variations of 2D or 3D channel geometries and/or manipulation of shear stress to control fluid flow rates (Figure 6a).<sup>[3,8,224,236,237,238]</sup> A variety of substrate materials have been used for fabrication of microfluidic devices, most common of which are PDMS, poly-methyl methacrylate, poly-vinyl alcohol, and polytetrafluoroethylene (Teflon).<sup>[258,259]</sup> T-junction, co-axial, and flow-focusing channel geometries are the most commonly used designs, all of which can be operated to enable fluid segmentation by dripping or jetting.<sup>[237,260]</sup> Furthermore, the physicochemical properties of the reagents dictate if the channels need to be patterned in 2D or 3D. In few cases, partially 3D channels have also been used.<sup>[261]</sup>

Emulsion-based microgel fabrication involves breaking the aqueous gel precursor solutions into discrete volumes by a (immiscible) solution in the dispersed phase;<sup>[3,262]</sup> thus generated microparticles undergo gelation to establish solid networks.<sup>[263]</sup> Gelation of microparticles can be controlled to occur internally, using gelation agents within the droplet, or externally. Externally, they can be made during on-chip mixing of precursor solutions and gelation agent, in an on-chip reservoir, in a downstream processing solution containing gelation agent, or in double emulsions.<sup>[14,258]</sup> The choice of material is dictated by biocompatibility, gelation time of precursor solutions, rate of recovery of microparticles, chip-resistance, and pregelation clogging.<sup>[14]</sup>

PDMS-based chips have been widely used, as it is feasible to generate many identical devices from the same master.<sup>[27,264]</sup> There have been studies on PDMS microfluidic devices comprising two individual flow focusing channels for the synthesis of various polymeric-shaped alginate microgels (rods, fibers, spheres, etc.).<sup>[265]</sup> A PDMS-glass hybrid device with a T-channel combined with a downstream Y-channel is used to synthesize Janus alginate hydrogel particles with magnetic anisotropy.<sup>[266]</sup> A three-layer T-junction (polymethyl methacrylate) microfluidic assembly has been used to fabricate tail-shaped alginate microparticles to investigate controlled drug release.<sup>[57]</sup> Additionally, the viscosity of the alginate solution affects both the length and diameter of the microparticle, with lower viscosity resulting in reduced dimensions.<sup>[57]</sup>

## 8.2. Capillary Microfluidics

Capillary microfluidic devices consist of circular glass capillaries placed with bigger capillaries in a co-axial manner (Figure 6b). This is achieved by matching the outer diameter of the inner circular capillary to the inner dimensions of the outer square capillary. Capillary microfluidics has been used to generate thermosensitive PNIPAM microgels embedded with a variety of internal morphologies containing embedded particles, voids, or core-shell structures.<sup>[239,267]</sup> These device designs can be modified by combining multiple microcapillary devices in series in a multistaged emulsion set up to produce microgels and microshells with multiphase cores.<sup>[268]</sup> In capillary fluid devices, the size of the microgels can be controlled using relative flow rates and orifice sizes.

In one study, a circular glass capillary is heated and pulled using a pipette puller to create the required tapered geometry with a fine orifice.<sup>[269]</sup> The dispersed phase consisted of aqueous NIPAM monomer, a cross-linking monomer *N,N'*-methylenebisacrylamide<sup>[338]</sup> and an ammonium persulfate initiator, while kerosene with/without dissolved reaction accelerator *N,N,N',N'*-tetramethylethylenediamine (TEMED) is used as the continuous phase. This study enables diffusion of TEMED from the oil phase into the aqueous phase to trigger a redox cross-linking reaction resulting in polymerization of PNIPAM microgels. Additionally, microgels with spherical voids formed by selectively dissolving previously embedded polystyrene particles of varying sizes.<sup>[269]</sup>

The glass-capillary method can also be used for the generation of monodisperse microgels embedded with fluorescently labeled polystyrene particles, quantum dots, or magnetic particles.<sup>[267]</sup> The particles are suspended in the aqueous monomer mixture. As these particles are physically trapped in the microgels, their addition has no adverse effect on gelation or thermosensitive behavior of the microgels. The same device setup has also been used to produce PNIPAM microcapsules with a core-shell structure by using inner and outer fluids which are immiscible with the middle fluid.<sup>[267]</sup>

## 8.3. Other Fabrication Methods

Electrospray is another method used to fabricate microparticles with tunable sizes and variable compositions, especially for the generation of monodisperse, all-aqueous microparticles from a broad range of viscous solutions (Figure 6c).<sup>[240,241,270]</sup> An all-aqueous electrospray approach has been developed to generate monodisperse single and double emulsion droplets, resulting in the synthesis of microsphere particles and core-shell structures.<sup>[241]</sup> The technique demonstrates the use of water/water core-shell dextran-in-PEG droplets as templates for the formation of porous collagen microspheres, calcium-alginate particles, and collagen-shelled capsules.<sup>[240,241,270]</sup> Therefore, it is a versatile and robust platform for use of different gelation schemes, for instance photopolymerization, thermal gelation, and chemical cross-linking.<sup>[241]</sup>

Microgels can also be fabricated from micro molds or wells, or by the photo-cross-linking of microgels under a patterned mask (Figure 6d).<sup>[242–244]</sup> For example, cubic or triangular-prism shaped microgels are fabricated under a mask with predesigned patterns in UV light. The non-cross-linked material is flushed away after microgel formation.<sup>[271]</sup> By changing the shape of the wells or mask, microgels with different shapes can be made and parts of these microgels can be coated.<sup>[243]</sup> Spiral microgels can be generated in this way using the thermoresponsive behavior of the material.<sup>[243]</sup>

A rapid and simple method to produce microparticles is by exposing microgel precursor solutions to shear or rotational stress in a continuous phase containing surfactants. For example, alginate microparticles internally gelled and emulsified in oil have been generated by centrifugal forces using an impeller and rotational speed.<sup>[272]</sup> The size range of the microgel is controlled by the intensity of the shear force applied.<sup>[122]</sup> While this method is easily scalable, it does

result in heterogeneous distribution of particle sizes, in the case of the alginate microparticles ranging between 200 and 1000  $\mu\text{m}$ .<sup>[272]</sup> In another study, PEG microgels are formed by exposing a mixture of the aqueous solution and a continuous phase to shear stress by either vortexing (low shear) or sonication (high shear) (Figure 6e).<sup>[122]</sup> These microgels are later co-assembled with cells to form 3D cell-laden microporous scaffolds.<sup>[122]</sup>

Another method for microgel production is LLPS (Figure 6f). First, polymers are dissolved, forming a homogeneous solution. Then, the saturation concentration is decreased, for example, by adding salt, changing pH, or changing the temperature.<sup>[59,66]</sup> Some of the biopolymers will then not be able to stay dissolved in solution and will form another phase, a solute-rich phase, which will be the engineered microgels.<sup>[59,273]</sup> LLPS can occur for synthetic copolymers and extracellular proteins, including ones used in natural structural materials.<sup>[274,275]</sup> Using LLPS in various continuous phases is a promising method of generating microgels, though the monodispersity of microgels is challenging to achieve.<sup>[21,59,245–247,273–275]</sup>

#### 8.4. Surface Functionalization

The surfaces of microgels can be modified at various fabrication stages to achieve specific functions. The amino acids on the microgel surfaces could be used to glue microgels for the formation of larger constructs of complex shapes.<sup>[127]</sup> For example, the surfaces of microgels with K and Q peptides are connected in the presence of activated Factor XIII via a noncanonical amide linkage.<sup>[127]</sup> Through the sol–gel transition (polycondensation reaction), silica hydrogel layers with cells are coated on the surfaces of preformed GelMA microgels.<sup>[276]</sup> Such coating method could protect the biological structures against oxidative stress *in vitro* and *in vivo*.<sup>[276]</sup> Amphiphilic Janus microgels with hydrophilic and hydrophobic components are generated using polyethylene and polypropylene materials, resulting in a hydrogel–organogel hybrid.<sup>[277]</sup> The combination of hydrophilic and hydrophobic parts can selectively allow the water or oil uptake of the microgels, and the directional arrangement of the microgels at water–oil interfaces.<sup>[277]</sup>

#### 8.5. Tailoring Functionality and Targeted Release

One avenue to include functionality into microgels is to modify the scaffold macromolecules. For example, Arg-Gly-Asp motifs can promote cell attachment or immobilization, and are incorporated into microgels for following cell-culture studies that require the adhesion of cells to microgel materials such as PEG or alginate.<sup>[29,143,278]</sup> Transglutaminase has been loaded with or uptaken by gelatin to form enzymatically cross-linked microgels which are more thermostable than physically cross-linked microgels.<sup>[3,279]</sup> A fundamentally different approach to include functional components is through using microgels as carriers to load cargoes such as nanoparticles, proteins, small molecules, nucleic acids, and cells.<sup>[3,153,154]</sup> These payloads can later be released at some time point to achieve certain functions, for example, for gene delivery (Section 6.1).<sup>[153,154]</sup>

#### 8.6. Scalable Manufacturing Challenges and Opportunities

A key challenge for the industrial application of microgels is achieving efficient mass production with high levels of reproducibility. This is an active area and several innovative approaches have emerged in the recent years. For example, a particle replication in nonwetting technique is developed to produce uniform-sized microgels (Figure 6g), which holds potential for drug carriers or drug particles.<sup>[248–250]</sup> The use of fluoropolymer molds can guide the formation of nonspherical and shape-specific microgels.<sup>[248,280]</sup> A parallel microfluidic chip (step emulsification) has been developed to address the growing demand of microdroplets;<sup>[251]</sup> there are multiple parallel inlets for dispersed phase and one inlet for the continuous phase, and droplets form during the Rayleigh–Plateau-type instability.<sup>[251]</sup> The step emulsification is further studied with the buoyancy of droplets (Figure 6h), which avoids the droplet accumulation in the channels and preserves the droplet monodispersity.<sup>[252]</sup> The development of the scale-up of droplet generation would eventually benefit the pharmaceutical, healthcare, and environment protection industries.

### 9. Surfactants and Demulsification of the Microdroplets

Various oil/surfactant systems have been used for the formation of microgels or microdroplets (Table 2).<sup>[3–5,8,27,281,282]</sup> In this section, we will discuss the factors to consider when choosing an oil, surfactant, or demulsifier. When choosing an oil which will be used at elevated temperatures, the stability of different oils should be compared.<sup>[281]</sup> In practice, fluorocarbon oil can be more clear under microscopes; however, the hydrocarbon oil systems are more economically and environmentally friendly. Using a fluorocarbon surfactant will result in a lower surface tension than hydrocarbon surfactants, and fluorocarbon surfactants can be used at lower concentrations. Fluorocarbon surfactants are also stable in extreme environments, and usually compatible with other surfactants.<sup>[281]</sup> As the most electronegative element, fluorine has made the bond energy of C–F bond higher than the C–H bond; also the polarity of C–F bond is lower than the C–H bond, which contributes to both an increased hydrophobicity and lipophobicity of fluorocarbon chains.<sup>[281,283]</sup>

When choosing a surfactant, it is important to consider the critical micelle concentration, the electrostatic interaction between biomolecules and surfactants, the optical properties, wetting properties, the thermal resistance, price, and feasibility for micelles or the reversed micelles.<sup>[283,284]</sup> The size and scale of the droplets, the hydrophilicity of the encapsulated molecules, the ionic concentration and the pH of the aqueous phase can also trigger the instability of emulsions. In one study, decreasing microgel size has been observed with increasing concentration of surfactant;<sup>[285]</sup> and nanogels could be obtained when higher amount of surfactant is used.<sup>[285]</sup> In another study, combined oils and combined surfactants are used for water/oil emulsion, and the volume fraction of oils and the fraction of surfactants are deterministic factors of the contact angle, offering possibilities of the controlled packing of droplets as

synthetic tissues.<sup>[286]</sup> Biocompatible fluorosurfactants that can inhibit the uncontrolled adsorption of proteins at the interfaces have been developed.<sup>[281,287]</sup> In cases where cargoes are expected to be fully encapsulated, the surfactant layer should be stable enough.<sup>[287]</sup> The type, ratio, concentration, and composition of surfactants should thus be systematically recorded for microfluidics and emulsions. Surfactants usually contain a hydrophilic and lipophilic region, and can modify the interfacial properties at low concentrations.<sup>[283]</sup> The applications and characteristics of these amphiphilic compounds vary based on not only the organic chains but also the polar groups, and thus the surfactants could be nonionic, anionic, cationic, and zwitterionic.<sup>[288]</sup>

The adsorption and orientation of the surfactants contribute to the stabilization of the emulsions and should thus be considered for the applications of surfactants.<sup>[289]</sup> Water-in-oil or oil-in-water droplets can be obtained with suitable surfactants. Surfactants are similar in structure to the lipids making up cellular membranes and have been used in applications like micelles, lipid-like bilayers, gelation, temperature-controlled phase transformation, concentration induced stress, and photocuring.<sup>[290,291]</sup> Surfactants can be nonessential in the situations where microdroplets can be gelated in the outlet tubing,<sup>[292]</sup> or where protein nanofibrils at all-aqueous interfaces are used.<sup>[240,270]</sup>

Demulsifiers are able to irreversibly separate the aqueous phase (hydrogels) from the oil phase (Table 3).<sup>[2,3]</sup> Table 3 shows the common methods of the demulsification of microgels, in order to finally rinse the microgels in an aqueous solution; such methods usually involve physical forces and chemical reagents. Owing to the potential impacts of surfactants and demulsifiers on the biomolecules as well as the cost, other methods free from surfactants and demulsifiers, such as the formation of all-aqueous emulsion and the rapid exchange of continuous phase, have been developed.<sup>[240,241,270,293–299]</sup>

## 10. Characterization Approaches of the Microgels

Multiple techniques and tools have been adopted or applied to characterize the microgels, including the morphology, content, conformation, degradability, mechanical properties, sol–gel transition, biocompatibility, the kinetics of protein aggregation, and drug release (Figure 7 and Table 4).

Optical microscopy is one of the most common methods used to characterize microgels. For example, bright-field images showed the gelatin microgels in oil or PBS, and pseudo bright-field images showed the hole–shell microgels and buckled microcapsules (Figure 7a).<sup>[8]</sup> As a complement, fluorescent images could indicate the distribution of the fluorophores in the microgels. The release of the fluorophores can be used to indicate the digestion of the microgels. Protein fibril and the conformation of protein inside them can be directly visualized with confocal microscopy and cross-polarization microscopy (Figure 7b).<sup>[1]</sup>

Electron microscopy has also been used for the observation and analysis of the microgels. With a scanning electron microscope (SEM), the information of the surface, and the internal nanoporous structures are easily accessible. Proper sample treatment methods are crucial for obtaining reliable results

as microgel samples can shrink slightly during sample treatment (Figure 7c).<sup>[59]</sup> In addition, energy dispersive spectroscopy has also been applied to couple the chemical components with morphological information, which is useful to quantitatively determine the inhomogeneity of the microgels.<sup>[300]</sup> Transmission electron microscopy (TEM) is also a powerful approach to determine the morphology of the microgels, particularly to determine fibril structures that compose the microgels, and information about nanoparticles can also be gathered through TEM (Figure 7d).<sup>[301]</sup>

Transmission X-ray microscopy is used for the characterization of the microgels, for example, for the z-stack imaging and 3D reconstruction.<sup>[302]</sup> The thermosensitive radial profiles of microgels in aqueous environments can be obtained in a scanning soft X-ray transmission microscopy, and the deswelling of the microgels can be analyzed digitally.<sup>[303]</sup> Small-angle X-ray scattering (SAXS) can be used to determine the shape and the structural transition of biological molecules,<sup>[304,305]</sup> and the structural evolution during microgel-to-particle collapse indicate there is a hollow structure in between. As a complement of SAXS, small angle neutron scattering (SANS) can also function as a simple way to employ contrast variation for unique information in microgel studies.<sup>[306–308]</sup> Wide-angle X-ray scattering (WAXS) is used for the illustration of the formation of Zn-based metal–organic framework ZIF-8 networks.<sup>[309]</sup>

Microfluidic chips are also used as characterization tools. For example, a microgel-trapping microfluidic chip are used to quantify the force generated during the polymerization of the amyloid fibrils (Figure 7e).<sup>[120]</sup> Additionally, microfluidic chips are used to quantify the elastic modulus of microgels in tapering microfluidic channels;<sup>[310]</sup> this concept has also been used to trigger and locate shearing-induced gelation of protein at an even smaller scale.<sup>[59]</sup>

Glass capillaries have been used for the storage of droplets, since this can prevent the evaporation of droplets and allow the long-term preservation and observation of the droplets (Figure 7f).<sup>[217,311]</sup> Tapered glass microcapillaries are used to determine both the compressive and the shear moduli of microgels in one experiment.<sup>[86]</sup> The principles of squeezed microgels entrancing into smaller capillaries are also explored, which has implications for situations such as occlusion of blood vessels by thrombi and needle-assisted hydrogel injection in tissue engineering.<sup>[312]</sup>

With UV spectroscopy and Fourier transform infrared spectroscopy (FTIR), the structural changes of the silk protein during the formation of microcapsules with varying shapes and the release properties of antibodies are also analyzed.<sup>[1]</sup> The enzymatic activity of protein fibrils within the microgel droplets can also be monitored with fluorescent substrates, which show the potential of slow release or targeted delivery of small molecules or other bioactive molecules in a high-throughput fashion.<sup>[216]</sup>

Secondary structures of protein aggregates are also of interest for the formation of microgels. Circular dichroism (CD) is used to determine the content of the final  $\beta$ -sheet in microgels.<sup>[53]</sup> CD analyses make it possible to study the degree of aggregation of the lysozyme protein, and no significant difference in  $\beta$ -sheet content is found between fibrillar lysozyme in bulk and microgels.<sup>[220]</sup>

The morphology of protein fibrils is characterized by AFM and TEM,<sup>[216]</sup> showing the dense mesh-like networks in microdroplets, individual amyloid fibrils, and small aggregates in a solution of protein. Lysozyme monomers, seeds, fibrils, and microgels are also analyzed by AFM on mica slides, which laid the foundation of seed-dependent protein fibrillization in combination with fluorescent confocal microscopy (Figure 7g).<sup>[220]</sup>

FTIR analysis can explain the transformation of monomeric lysozyme into nanofibrillar structures, both in bulk and in microgels, which contribute to the understanding of the difference of  $\beta$ -sheet contents from lysozyme fibers, microgels, and monomers.<sup>[220]</sup> FTIR measurements also determine the change in protein structure of bulk samples under shear stress, showing a change of content of parallel  $\beta$ -sheet,  $\alpha$ -helix, antiparallel  $\beta$ -sheet, and random coils.<sup>[59]</sup>

It has been interesting to study the sol–gel transition of materials at the microscale, and fluorescence recovery after photobleaching (FRAP) is one of the most promising approaches to explore the sol or gel behaviors, utilizing the diffusion of a substance. The mobility of lysozyme can be studied in starch microgels at different salt and pH concentrations with FRAP.<sup>[313]</sup> Diffusion of fluorescently tagged linear macromolecules by FRAP at the microscale is carried out in addition to rheology.<sup>[314]</sup> The sol–gel transition of protein condensates undergoing various shear stress is also explored by FRAP (Figure 7h).<sup>[59]</sup>

For “small” microgels in the scale of nanometer or submicron, super-resolution fluorescence microscopy (SRFM) and AFM have been advantageous in the characterization.<sup>[18–24]</sup> SRFM can be an effective imaging method in combination with precise labeling protocols, when other imaging methods require harsh sample preparation or produce poor contrast of small microgels.<sup>[18–21]</sup> The mechanical properties (complex modulus) of “small” microgels can be measured at high resolution as a result of the fine size of the AFM tips, and the measurement can be conducted in aqueous environment.<sup>[22–24]</sup> For example, deformation, stiffness, and apparent elastic modulus of microgels have been explored for temperature-dependent nanomechanics with AFM.<sup>[23]</sup>

## 11. Summary and Outlook

This review summarizes the common structures of homogeneous, inhomogeneous, and heterogeneous microgels, the diversity of natural materials for microgels, the fabrication and formulation of the microgels, the characterization of the microgels, and the applications of the microgels including LLPS, micromechanics, biosensing, and regenerative medicine. Microgel models are potent in these application areas, which are closely related to functional and smart materials, devices, or structures. The development of hydrogels that are inhomogeneous or heterogeneous at the molecular, nano-, micro-, meso-, and/or macro-scale has been the significant focus of the research.<sup>[14]</sup> Microgels are useful carriers connecting a broad range of length scales, particularly for healthcare and medicine. To broaden the application scenarios of these microgels and to better contribute to healthcare fields, it is worthwhile conducting more research in the following areas such as the scale-up of the production of the microgels, the improvement

of the biocompatibility and biomimicry of the microgels, and consideration of green chemistry and energy consumption throughout the production in labs or industries.

### 11.1. Green Chemistry and Sustainable Manufacturing

In consideration of current environmental challenges, it is necessary to adopt technologies that are in line with green chemistry as far as possible. The production of microgels is usually involved with chemical reagents, manufacturing platforms, and/or industrial routines. The disposal of microgels should also be considered. Thus, the sustainability footprint of microgels should reflect the utilization of a range of principles for the benefit of the environment and our planet. The use of natural materials and synthetic polymers should be balanced, considering the overall environmental burdens.<sup>[321]</sup> When making protein microgels, plant-based materials and animal-based materials should also be well assessed.<sup>[92]</sup> The energy consumption in the manufacturing and the recyclability of the microfluidic chips, compounded by the use of chips in parallel, could promote the rational design of fabrication methods of the microgels.<sup>[137,322]</sup> Microgels that are easily degradable and generated from biocompatible and biodegradable building blocks are critical components in future renewable materials systems and are environmentally friendly, as they emit no or few microplastic wastes into the ocean or soil.

### 11.2. Training the Microgels

Applying microgels to biological scenarios under dynamic conditions is another trend of bioengineering and biomedicine, which is similar to the training of muscles in a gym. External environmental stimuli, such as mechanical pressure, magnetic field, and chemical cues, could trigger the internal changes of the microgels, and thus could influence the cells or molecules trapped in the microgels.<sup>[8,87,323,324]</sup> advanced microgel models can thus be trained dynamically to achieve certain time-dependent research purposes. For example, artificial tissues under mechanical stress can be simulated in vitro.<sup>[325–327]</sup> It is possible to study the ageing of proteins under different physicochemical factors.<sup>[59]</sup> The aggregation, fusion, and degradation of microgels could also inspire the emergence of on-demand training approaches. Relevant auxiliary platforms, such as bioreactors or mixers, microfluidic trapping, and precise force generators, should be developed along with the progress of microgels for biological applications.

### 11.3. Antiviral Microgels and Vaccine Development

Microgels have enormous potential to function as bioreactors, biosensors, and adsorption sites, as a result of their miniaturized, hydrated, and porous compartments at the microscale. The current Covid-19 pandemic emphasizes the need of antiviral therapies and preventions against SARS-Cov-2 and other viruses. Microgels can play roles in drug delivery or release, controllable degradability, and stimuli-responsive

behaviors;<sup>[3,4,8,328–330]</sup> it can therefore be forecast that microgels could be applied to the carriers of the antiviral drugs or sensors.<sup>[321,331–333]</sup> Such drug-laden microgels could release the payloads at controlled rates, either in a fast or in a gradual fashion.<sup>[332]</sup> Studies have been conducted to test the potential application of hydrogels in antiviral water filtration system. Inspired by that, microgels could serve as a new class of sterilizing materials in the future.<sup>[321,334,335]</sup> Other significant studies on viruses, such as antigen–antibody interactions, gene delivery, vaccine development, sensing, lipid nano particle efficiency, and virus mutations, could also be explored with microgel models.<sup>[150,336,337]</sup>

## Acknowledgements

Y.X. and H.Z. contributed equally to this work. The research leading to these results had received funding from the Cambridge Trust (Y.X.), the Jardine Foundation (Y.X.), Trinity College Cambridge (Y.X.), the China Scholarship Council (H.Z.), the Bill and Melinda Gates Foundation (A.D.), the Royall Scholarship (N.A.E.), the Trinity College Krishnan-Ang Studentship (R.Q.), the Honorary Trinity-Henry Barlow Scholarship (R.Q.), the BBSRC (T.P.J.K.), the Newman Foundation (T.P.J.K.), the Wellcome Trust (T.P.J.K.), and the European Research Council under the European Union's Seventh Framework Programme (FP7/2007–2013) through the ERC grant PhysProt (agreement no. 337969; T.P.J.K.). T.P.J.K. is a founder of Xampla Ltd.

## Conflict of Interest

The authors declare no conflict of interest.

## Keywords

3D cell cultures, biomolecules, biosensing, characterization, fabrication, liquid–liquid phase separation, microgels, micromechanics

Received: January 10, 2022

Revised: March 15, 2022

Published online:

- [1] U. Shimanovich, F. S. Ruggeri, E. De Genst, J. Adamcik, T. P. Barros, D. Porter, T. Müller, R. Mezzenga, C. M. Dobson, F. Vollrath, C. Holland, T. P. J. Knowles, *Nat. Commun.* **2017**, *8*, 15902.
- [2] A. S. Mao, J.-W. Shin, S. Utech, H. Wang, O. Uzun, W. Li, M. Cooper, Y. Hu, L. Zhang, D. A. Weitz, D. J. Mooney, *Nat. Mater.* **2017**, *16*, 236.
- [3] Y. Xu, R. P. B. Jacquat, Y. Shen, D. Vigolo, D. Morse, S. Zhang, T. P. J. Knowles, *Small* **2020**, *16*, 2000432.
- [4] Y. Xu, R. Qi, H. Zhu, B. Li, Y. Shen, G. Krainer, D. Klenerman, T. P. J. Knowles, *Adv. Mater.* **2021**, *33*, 2008670.
- [5] C. B. Highley, K. H. Song, A. C. Daly, J. A. Burdick, *Adv. Sci.* **2019**, *6*, 1801076.
- [6] Y. Pan, Y. Qi, X. Li, S. Luan, Y. Huang, *Adv. Funct. Mater.* **2021**, *31*, 2105742.
- [7] C. C. Cutright, J. L. Harris, S. Ramesh, S. A. Khan, J. Genzer, S. Menegatti, *Adv. Funct. Mater.* **2021**, *31*, 2104164.
- [8] Y. Xu, Y. Shen, T. C. T. Michaels, K. N. Baumann, D. Vigolo, Q. Peter, Y. Lu, K. L. Saar, D. Vella, H. Zhu, B. Li, H. Yang,

- A. P. M. Guttenplan, M. Rodriguez-Garcia, D. Klenerman, T. P. J. Knowles, *Adv. Mater. Interfaces* **2021**, *8*, 2101071.
- [9] Z. Zhao, Z. Wang, G. Li, Z. Cai, J. Wu, L. Wang, L. Deng, M. Cai, W. Cui, *Adv. Funct. Mater.* **2021**, *31*, 2103339.
- [10] H. Qi, Y. Du, L. Wang, H. Kaji, H. Bae, A. Khademhosseini, *Adv. Mater.* **2010**, *22*, 5276.
- [11] S. Ma, N. Mukherjee, E. Mikhailova, H. Bayley, *Adv. Biosyst.* **2017**, *1*, 1700075.
- [12] X. Yan, J. C. M. van Hest, *Chem. - Asian J.* **2018**, *13*, 3331.
- [13] L. Zhao, G. Shen, G. Ma, X. Yan, *Adv. Colloid Interface Sci.* **2017**, *249*, 308.
- [14] W. Li, L. Zhang, X. Ge, B. Xu, W. Zhang, L. Qu, C.-H. Choi, J. Xu, A. Zhang, H. Lee, D. A. Weitz, *Chem. Soc. Rev.* **2018**, *47*, 5646.
- [15] Q. Feng, D. Li, Q. Li, X. Cao, H. Dong, *Bioact. Mater.* **2022**, *9*, 105.
- [16] A. S. Mao, B. Özkale, N. J. Shah, K. H. Vining, T. Descombes, L. Zhang, C. M. Tringides, S.-W. Wong, J.-W. Shin, D. T. Scadden, D. A. Weitz, D. J. Mooney, *Proc. Natl. Acad. Sci. U. S. A.* **2019**, *116*, 15392.
- [17] A. A. Karanastasis, Y. Zhang, G. S. Kenath, M. D. Lessard, J. Bewersdorf, C. K. Ullal, *Mater. Horiz.* **2018**, *5*, 1130.
- [18] G. M. Conley, P. Aebischer, S. Nöjd, P. Schurtenberger, F. Scheffold, *Sci. Adv.* **2017**, *3*, e1700969.
- [19] S. Bergmann, O. Wrede, T. Huser, T. Hellweg, *Phys. Chem. Chem. Phys.* **2018**, *20*, 5074.
- [20] E. Siemes, O. Nevskiy, D. Sysoiev, S. K. Turnhoff, A. Oppermann, T. Huhn, W. Richtering, D. Wöll, *Angew. Chem., Int. Ed.* **2018**, *57*, 12280.
- [21] W. Xu, A. Rudov, A. Oppermann, S. Wypsek, M. Kather, R. Schroeder, W. Richtering, I. I. Potemkin, D. Wöll, A. Pich, *Angew. Chem., Int. Ed.* **2020**, *59*, 1248.
- [22] S. Backes, R. Von Klitzing, *Polymers* **2018**, *10*, 978.
- [23] G. Li, I. Varga, A. Kardos, I. Dobryden, P. M. Claesson, *J. Phys. Chem. B* **2021**, *125*, 9860.
- [24] M. F. Schulte, S. Bochenek, M. Brugnoli, A. Scotti, A. Mourran, W. Richtering, *Angew. Chem., Int. Ed.* **2021**, *60*, 2280.
- [25] Y. Hu, G. Azadi, A. M. Ardekani, *Carbohydr. Polym.* **2015**, *120*, 38.
- [26] W. Wang, M.-J. Zhang, R. Xie, X.-J. Ju, C. Yang, C.-L. Mou, D. A. Weitz, L.-Y. Chu, *Angew. Chem., Int. Ed.* **2013**, *52*, 8084.
- [27] T. P. J. Knowles, D. A. White, A. R. Abate, J. J. Agresti, S. I. A. Cohen, R. A. Sperling, E. J. De Genst, C. M. Dobson, D. A. Weitz, *Proc. Natl. Acad. Sci. U. S. A.* **2011**, *108*, 14746.
- [28] L. P. B. Guerzoni, J. C. Rose, D. B. Gehlen, A. Jans, T. Haraszti, M. Wessling, A. J. C. Kuehne, L. De Laporte, *Small* **2019**, *15*, 1900692.
- [29] A. J. D. Krueger, O. Bakirman, L. P. B. Guerzoni, A. Jans, D. B. Gehlen, D. Rommel, T. Haraszti, A. J. C. Kuehne, L. De Laporte, *Adv. Mater.* **2019**, *31*, 1903668.
- [30] D. Suzuki, C. Kobayashi, *Langmuir* **2014**, *30*, 7085.
- [31] X. Liang, Y. Deng, X. Pei, K. Zhai, K. Xu, Y. Tan, X. Gong, P. Wang, *Soft Matter* **2017**, *13*, 2654.
- [32] M. Brugnoli, A. Scotti, A. A. Rudov, A. P. H. Gelissen, T. Caumanns, A. Radulescu, T. Eckert, A. Pich, I. I. Potemkin, W. Richtering, *Macromolecules* **2018**, *51*, 2662.
- [33] S. Seiffert, J. Thiele, A. R. Abate, D. A. Weitz, *J. Am. Chem. Soc.* **2010**, *132*, 6606.
- [34] G. Hong, J. Kim, H. Oh, S. Yun, C. M. Kim, Y.-M. Jeong, W.-S. Yun, J.-H. Shim, I. Jang, C.-Y. Kim, S. Jin, *Adv. Mater.* **2021**, *33*, 2102624.
- [35] B. Haney, J. G. Werner, D. A. Weitz, S. Ramakrishnan, *Soft Matter* **2020**, *16*, 3613.
- [36] S. Seiffert, D. A. Weitz, *Polymer* **2010**, *51*, 5883.
- [37] S. Seiffert, M. B. Romanowsky, D. A. Weitz, *Langmuir* **2010**, *26*, 14842.
- [38] S. Kühn, J. Sievers, A. Stoppa, N. Träber, R. Zimmermann, P. B. Welzel, C. Werner, *Adv. Funct. Mater.* **2020**, *30*, 1908857.

- [39] H. Xie, Z.-G. She, S. Wang, G. Sharma, J. W. Smith, *Langmuir* **2012**, *28*, 4459.
- [40] O. B. Garbuzenko, J. Winkler, M. S. Tomassone, T. Minko, *Langmuir* **2014**, *30*, 12941.
- [41] S. Y. Kashani, A. Afzalian, F. Shirinichi, M. K. Moraveji, *RSC Adv.* **2021**, *11*, 229.
- [42] T. C. Le, J. Zhai, W.-H. Chiu, P. A. Tran, N. Tran, *Int. J. Nanomed.* **2019**, *14*, 6749.
- [43] G. Agrawal, R. Agrawal, A. Pich, *Part. Part. Syst. Charact.* **2017**, *34*, 1700132.
- [44] D. Rommel, M. Mork, S. Vedaraman, C. Bastard, L. P. B. Guerzoni, Y. Kittel, R. Vinokur, N. Born, T. Haraszti, L. De Laporte, *Adv. Sci.* **2022**, *9*, 2270060.
- [45] A. M. Mihut, B. Stenqvist, M. Lund, P. Schurtenberger, J. J. Crassous, *Sci. Adv.* **2017**, *3*, e1700321.
- [46] Y. Du, E. Lo, S. Ali, A. Khademhosseini, *Proc. Natl. Acad. Sci. U. S. A.* **2008**, *105*, 9522.
- [47] A. S. Caldwell, B. A. Aguado, K. S. Anseth, *Adv. Funct. Mater.* **2020**, *30*, 1907670.
- [48] Y. Hu, Q. Wang, J. Wang, J. Zhu, H. Wang, Y. Yang, *Biomicrofluidics* **2012**, *6*, 026502.
- [49] R. Jenjob, T. Phakkeeree, D. Crespy, *Biomater. Sci.* **2020**, *8*, 2756.
- [50] S. Argenti, P. A. Sciliano, L. Blasi, *Polymers* **2021**, *13*, 3216.
- [51] Q. Chen, S. Utech, D. Chen, R. Prodanovic, J.-M. Lin, D. A. Weitz, *Lab Chip* **2016**, *16*, 1346.
- [52] L. Zhang, K. Chen, H. Zhang, B. Pang, C.-H. Choi, A. S. Mao, H. Liao, S. Utech, D. J. Mooney, H. Wang, D. A. Weitz, *Small* **2018**, *14*, 1702955.
- [53] U. Shimanovich, Y. Song, J. Brujic, H. C. Shum, T. P. J. Knowles, *Macromol. Biosci.* **2015**, *15*, 501.
- [54] S. Minami, D. Suzuki, K. Urayama, *Curr. Opin. Colloid Interface Sci.* **2019**, *43*, 113.
- [55] Y. Shen, A. Levin, A. Kamada, Z. Toprakcioglu, M. Rodriguez-Garcia, Y. Xu, T. P. J. Knowles, *ACS Nano* **2021**, *15*, 5819.
- [56] T. P. J. Knowles, R. Mezzenga, *Adv. Mater.* **2016**, *28*, 6546.
- [57] Y.-S. Lin, C.-H. Yang, Y.-Y. Hsu, C.-L. Hsieh, *Electrophoresis* **2013**, *34*, 425.
- [58] Z. Toprakcioglu, P. K. Challa, A. Levin, T. P. J. Knowles, *Lab Chip* **2018**, *18*, 3303.
- [59] Y. Shen, F. S. Ruggeri, D. Vigolo, A. Kamada, S. Qamar, A. Levin, C. Iserman, S. Alberti, P. S. George-Hyslop, T. P. J. Knowles, *Nat. Nanotechnol.* **2020**, *15*, 841.
- [60] C. Yuan, M. Yang, X. Ren, Q. Zou, X. Yan, *Angew. Chem., Int. Ed.* **2020**, *59*, 17456.
- [61] S. Elbaum-Garfinkle, Y. Kim, K. Szczepaniak, C. C.-H. Chen, C. R. Eckmann, S. Myong, C. P. Brangwynne, *Proc. Natl. Acad. Sci. U. S. A.* **2015**, *112*, 7189.
- [62] S. Alberti, A. Gladfelter, T. Mittag, *Cell* **2019**, *176*, 419.
- [63] H. Sakuta, F. Fujita, T. Hamada, M. Hayashi, K. Takiguchi, K. Tsumoto, K. Yoshikawa, *ChemBioChem* **2020**, *21*, 3323.
- [64] Q. Ma, Y. Song, W. Sun, J. Cao, H. Yuan, X. Wang, Y. Sun, H. C. Shum, *Adv. Sci.* **2020**, *7*, 1903359.
- [65] W. E. Arter, R. Qi, G. E. Krainer, T. J. Welsh, Y. Xu, P. St George-Hyslop, S. Alberti, T. Knowles, *bioRxiv* **2020**, <https://doi.org/10.1101/2020.06.04.132308>.
- [66] G. Krainer, T. J. Welsh, J. A. Joseph, J. R. Espinosa, S. Wittmann, E. de Csilléry, A. Sridhar, Z. Toprakcioglu, G. Gudiskyte, M. A. Czekalska, W. E. Arter, J. Guillén-Boixet, T. M. Franzmann, S. Qamar, P. St George-Hyslop, A. A. Hyman, R. Collepardo-Guevara, S. Alberti, T. P. J. Knowles, *Nat. Commun.* **2021**, *12*, 1085.
- [67] C. Yuan, A. Levin, W. Chen, R. Xing, Q. Zou, T. W. Herling, P. K. Challa, T. P. J. Knowles, X. Yan, *Angew. Chem.* **2019**, *131*, 18284.
- [68] J. Wen, L. Hong, G. Krainer, Q.-Q. Yao, T. P. J. Knowles, S. Wu, S. Perrett, *J. Am. Chem. Soc.* **2021**, *143*, 13056.
- [69] H. Zhu, M. Narita, J. A. Joseph, G. Krainer, W. E. Arter, K. L. Saar, N. Ermann, J. R. Espinosa, Y. Shen, M. A. Kuri, R. Qi, Y. Xu, R. Collepardo-Guevara, M. Narita, T. P. J. Knowles, *bioRxiv* **2021**, <https://doi.org/10.1101/2021.10.14.464384>.
- [70] T. Liu, Y. Yin, Y. Yang, T. P. Russell, S. Shi, *Adv. Mater.* **2021**, *34*, 2105386.
- [71] S. D. Oberdick, G. Zabow, *ACS Appl. Polym. Mater.* **2020**, *2*, 846.
- [72] Y. Lan, A. Caciagli, G. Guidetti, Z. Yu, J. Liu, V. E. Johansen, M. Kamp, C. Abell, S. Vignolini, O. A. Scherman, E. Eiser, *Nat. Commun.* **2018**, *9*, 3614.
- [73] Y. Lan, J. Liu, E. Eiser, O. A. Scherman, *Polym. Chem.* **2019**, *10*, 3772.
- [74] H. U. Kim, D. G. Choi, Y. H. Roh, M. S. Shim, K. W. Bong, *Small* **2016**, *12*, 3463.
- [75] H. Liu, Y. Wang, K. Cui, Y. Guo, X. Zhang, J. Qin, *Adv. Mater.* **2019**, *31*, 1902042.
- [76] S. Jain, J. R. Wheeler, R. W. Walters, A. Agrawal, A. Barsic, R. Parker, *Cell* **2016**, *164*, 487.
- [77] J. A. West, M. Mito, S. Kurosaka, T. Takumi, C. Tanegashima, T. Chujo, K. Yanaka, R. E. Kingston, T. Hirose, C. Bond, A. Fox, S. Nakagawa, *J. Cell Biol.* **2016**, *214*, 817.
- [78] J. Fei, M. Jadhavi, T. S. Harmon, I. T. S. Li, B. Hua, Q. Hao, A. S. Holehouse, M. Reyer, Q. Sun, S. M. Freier, R. V. Pappu, K. V. Prasanth, T. Ha, *J. Cell Sci.* **2017**, *130*, 4180.
- [79] C. P. Brangwynne, T. J. Mitchison, A. A. Hyman, *Proc. Natl. Acad. Sci. U. S. A.* **2011**, *108*, 4334.
- [80] T. Kaur, M. Raju, I. Alshareedah, R. B. Davis, D. A. Potoyan, P. R. Banerjee, *Nat. Commun.* **2021**, *12*, 872.
- [81] M. Feric, N. Vaidya, T. S. Harmon, D. M. Mitrea, L. Zhu, T. M. Richardson, R. W. Kriwacki, R. V. Pappu, C. P. Brangwynne, *Cell* **2016**, *165*, 1686.
- [82] I. Alshareedah, M. M. Moosa, M. Raju, D. A. Potoyan, P. R. Banerjee, *Proc. Natl. Acad. Sci. U. S. A.* **2020**, *117*, 15650.
- [83] P. R. Banerjee, A. N. Milin, M. M. Moosa, P. L. Onuchic, A. A. Deniz, *Angew. Chem.* **2017**, *129*, 11512.
- [84] S. Dang, J. Brady, R. Rel, S. Surineni, C. O'Shaughnessy, R. McGorty, *Soft Matter* **2021**, *17*, 8300.
- [85] J. Wang, R. McGorty, *Bull. Am. Phys. Soc.* **2020**, *65*, 1.
- [86] H. M. Wyss, T. Franke, E. Mele, D. A. Weitz, *Soft Matter* **2010**, *6*, 4550.
- [87] Y. Xu, H. Zhu, Y. Shen, A. P. M. Guttenplan, K. L. Saar, Y. Lu, D. Vigolo, L. S. Itzhaki, T. P. J. Knowles, *MRS Bull.* **2022**, *47*, 119.
- [88] R. Kwok, E. Evans, *Biophys. J.* **1981**, *35*, 637.
- [89] F. S. Ruggeri, T. Šneideris, M. Vendruscolo, T. P. J. Knowles, *Arch. Biochem. Biophys.* **2019**, *664*, 134.
- [90] T. Kong, L. Wang, H. M. Wyss, H. C. Shum, *Soft Matter* **2014**, *10*, 3271.
- [91] M. Taffetani, X. Jiang, D. P. Holmes, D. Vella, *Proc. R. Soc. A* **2018**, *474*, 20170910.
- [92] A. Kamada, M. Rodriguez-Garcia, F. S. Ruggeri, Y. Shen, A. Levin, T. P. J. Knowles, *Nat. Commun.* **2021**, *12*, 3529.
- [93] T. P. J. Knowles, M. J. Buehler, *Nat. Nanotechnol.* **2011**, *6*, 469.
- [94] T. R. Cox, J. T. Erler, *Dis. Models Mech.* **2011**, *4*, 165.
- [95] H. Zhao, Z. Wang, S. Jiang, J. Wang, Z. Hu, P. E. Lobie, S. Ma, *Cell Rep. Phys. Sci.* **2020**, *1*, 100047.
- [96] J. Xu, G.-P. Shi, *Biochim. Biophys. Acta* **2014**, *1842*, 2106.
- [97] C. Bertulli, M. Gerigk, N. Piano, Y. Liu, D. Zhang, T. Müller, T. J. Knowles, Y. Y. S. Huang, *Sci. Rep.* **2018**, *8*, 12480.
- [98] Q. Wu, X. Wang, C. Liao, Q. Wei, Q. Wang, *Nanoscale* **2015**, *7*, 16578.
- [99] N. Sai, Z. Sun, Y. Wu, G. Huang, *Bioorg. Chem.* **2019**, *84*, 389.
- [100] L. V. Sigolaeva, S. Y. Gladys, O. Mergel, A. P. H. Gelissen, M. Noyong, U. Simon, D. V. Pergushov, I. N. Kurochkin, F. A. Plamper, W. Richtering, *Anal. Chem.* **2017**, *89*, 6091.

- [101] L. V. Sigolaeva, D. V. Pergushov, M. Oelmann, S. Schwarz, M. Brugnoli, I. N. Kurochkin, F. A. Plamper, A. Fery, W. Richtering, *Polymers* **2018**, 10, 791.
- [102] Q. M. Zhang, D. Berg, S. M. Mugo, M. J. Serpe, *Chem. Commun.* **2015**, 51, 9726.
- [103] E. Battista, F. Causa, P. A. Netti, *Gels* **2017**, 3, 20.
- [104] M. Wei, X. Li, M. J. Serpe, *ACS Appl. Polym. Mater.* **2019**, 1, 519.
- [105] S. Lin, Z. Wang, X. Chen, J. Ren, S. Ling, *Adv. Sci.* **2020**, 7, 1902743.
- [106] Q. Liu, S. Yang, J. Ren, S. Ling, *ACS Mater. Lett.* **2020**, 2, 712.
- [107] Z. Zhao, M. A. Al-Ameen, K. Duan, G. Ghosh, J. F. Lo, *Biosens. Bioelectron.* **2015**, 74, 305.
- [108] Y. Ma, X. Dai, T. Hong, G. B. Munk, M. Libera, *Analyst* **2017**, 142, 147.
- [109] K. Marcisz, K. Kaniewska, M. Mackiewicz, A. Nowinska, J. Romanski, Z. Stojek, M. Karbarz, *Electroanalysis* **2018**, 30, 2853.
- [110] A. Aliberti, A. M. Cusano, E. Battista, F. Causa, P. A. Netti, *Analyst* **2016**, 141, 1250.
- [111] Y. Gao, X. Li, M. J. Serpe, *RSC Adv.* **2015**, 5, 44074.
- [112] X. Li, Y. Gao, M. J. Serpe, *Gels* **2016**, 2, 8.
- [113] M. R. Islam, M. J. Serpe, *Anal. Bioanal. Chem.* **2014**, 406, 4777.
- [114] M. R. Islam, S. Azimi, F. Teimoori, G. Loppnow, M. J. Serpe, *Can. J. Chem.* **2018**, 96, 1079.
- [115] T. A. Hakala, F. Bialas, Z. Toprakcioglu, B. Bräuer, K. N. Baumann, A. Levin, G. J. L. Bernardes, C. F. W. Becker, T. P. J. Knowles, *ACS Appl. Mater. Interfaces* **2020**, 12, 32951.
- [116] L. V. Sigolaeva, S. Y. Gladys, A. P. H. Gelissen, O. Mergel, D. V. Pergushov, I. N. Kurochkin, F. A. Plamper, W. Richtering, *Biomacromolecules* **2014**, 15, 3735.
- [117] M. N. Holme, S. Rana, H. M. G. Barriga, U. Kauscher, N. J. Brooks, M. M. Stevens, *ACS Nano* **2018**, 12, 8197.
- [118] Y. Wang, V. Shah, A. Lu, E. Pachler, B. Cheng, D. Di Carlo, *Lab Chip* **2021**, 21, 3438.
- [119] Y. Jiang, M. G. Colazo, M. J. Serpe, *Anal. Bioanal. Chem.* **2018**, 410, 4397.
- [120] T. W. Herling, G. A. Garcia, T. C. T. Michaels, W. Grentz, J. Dean, U. Shimanovich, H. Gang, T. Müller, B. Kav, E. M. Terentjev, C. M. Dobson, T. P. J. Knowles, *Proc. Natl. Acad. Sci. USA* **2015**, 112, 9524.
- [121] X. Xia, X. Zhang, M. J. Serpe, Q. Zhang, *Adv. Mater. Technol.* **2020**, 5, 1900818.
- [122] A. S. Caldwell, G. T. Campbell, K. M. T. Shekiri, K. S. Anseth, *Adv. Healthcare Mater.* **2017**, 6, 1700254.
- [123] O. Jeon, Y. B. Lee, H. Jeong, S. J. Lee, D. Wells, E. Alsberg, *Mater. Horiz.* **2019**, 6, 1625.
- [124] T. H. Qazi, J. A. Burdick, *Biomater. Biosyst.* **2021**, 1, 100008.
- [125] J. C. Mejías, K. Roy, *J. Controlled Release* **2019**, 316, 393.
- [126] F. Li, C. Levinson, V. X. Truong, L. A. Laurent-Applegate, K. Maniura-Weber, H. Thissen, J. S. Forsythe, M. Zenobi-Wong, J. E. Frith, *Biomater. Sci.* **2020**, 8, 1711.
- [127] D. R. Griffin, W. M. Weaver, P. O. Scumpia, D. Di Carlo, T. Segura, *Nat. Mater.* **2015**, 14, 737.
- [128] S. R. Calia, J. A. Burdick, *Nat. Methods* **2016**, 13, 405.
- [129] O. Jeon, Y. B. Lee, T. J. Hinton, A. W. Feinberg, E. Alsberg, *Mater. Today Chem.* **2019**, 12, 61.
- [130] Q. Xu, P. Ying, J. Ren, N. Kong, Y. Wang, Y.-G. Li, Y. Yao, D. L. Kaplan, S. Ling, *Tissue Eng., Part B* **2020**, 27, 411.
- [131] B. M. Baker, C. S. Chen, *J. Cell Sci.* **2012**, 125, 3015.
- [132] S. Raghavan, C. J. Shen, R. A. Desai, N. J. Sniadecki, C. M. Nelson, C. S. Chen, *J. Cell Sci.* **2010**, 123, 2877.
- [133] J. E. Mealy, J. J. Chung, H.-H. Jeong, D. Issadore, D. Lee, P. Atluri, J. A. Burdick, *Adv. Mater.* **2018**, 30, 1705912.
- [134] J. M. de Rutte, J. Koh, D. Di Carlo, *Adv. Funct. Mater.* **2019**, 29, 1900071.
- [135] S. Allazetta, A. Negro, M. P. Lutolf, *Macromol. Rapid Commun.* **2017**, 38, 1700255.
- [136] D. M. Headen, K. B. Woodward, M. M. Coronel, P. Shrestha, J. D. Weaver, H. Zhao, M. Tan, M. D. Hunkler, W. S. Bowen, C. T. Johnson, L. Shea, E. S. Yolcu, A. J. García, H. Shirwan, *Nat. Mater.* **2018**, 17, 732.
- [137] D. M. Headen, J. R. García, A. J. García, *Microsyst. Nanoeng.* **2018**, 4, 17076.
- [138] S. Sart, R. F.-X. Tomasi, G. Amselem, C. N. Baroud, *Nat. Commun.* **2017**, 8, 469.
- [139] T. Kamperman, S. Henke, C. W. Visser, M. Karperien, J. Leijten, *Small* **2017**, 13, 1603711.
- [140] P. S. Lienemann, T. Rossow, A. S. Mao, Q. Vallmajo-Martin, M. Ehrbar, D. J. Mooney, *Lab Chip* **2017**, 17, 727.
- [141] H. Wang, H. Liu, H. Liu, W. Su, W. Chen, J. Qin, *Adv. Mater. Technol.* **2019**, 4, 1800632.
- [142] H. Wang, H. Liu, F. He, W. Chen, X. Zhang, X. Zhao, L. Wang, J. Qin, *Adv. Mater. Technol.* **2020**, 5, 2000045.
- [143] S. Allazetta, L. Kolb, S. Zerbib, J. Bardy, M. P. Lutolf, *Small* **2015**, 11, 5647.
- [144] C.-H. Choi, H. Wang, H. Lee, J. H. Kim, L. Zhang, A. Mao, D. J. Mooney, D. A. Weitz, *Lab Chip* **2016**, 16, 1549.
- [145] C. A. Lino, J. C. Harper, J. P. Carney, J. A. Timlin, *Drug Delivery* **2018**, 25, 1234.
- [146] C. Il Chang, T. Y. Lee, S. Kim, X. Sun, S. W. Hong, J. W. Yoo, P. Dua, H. S. Kang, S. Kim, C. J. Li, D. K. Lee, *J. Gene Med.* **2012**, 14, 138.
- [147] N. Bono, F. Ponti, D. Mantovani, G. Candiani, *Pharmaceutics* **2020**, 12, 183.
- [148] I. Lostalé-Seijo, J. Montenegro, *Nat. Rev. Chem.* **2018**, 2, 258.
- [149] J. Buck, P. Grossen, P. R. Cullis, J. Huwyler, D. Witzigmann, *ACS Nano* **2019**, 13, 3754.
- [150] B. G. Carvalho, F. F. Vit, H. F. Carvalho, S. W. Han, L. G. de la Torre, *Biomacromolecules* **2022**, 23, 1545.
- [151] B. S. Kaya, *Emergy Mater. Res.* **2020**, 9, 655.
- [152] R. Sunasee, P. Wattanaarsakit, M. Ahmed, F. B. Lollmahomed, R. Narain, *Bioconjugate Chem.* **2012**, 23, 1925.
- [153] J. M. Knipe, L. E. Strong, N. A. Peppas, *Biomacromolecules* **2016**, 17, 788.
- [154] S. A. Cohen, H. Simaan-Yameen, C. Fuoco, C. Gargioli, D. Seliktar, *Eur. Polym. J.* **2022**, 166, 111038.
- [155] G.-L. Ying, N. Jiang, S. Maharjan, Y.-X. Yin, R.-R. Chai, X. Cao, J.-Z. Yang, A. K. Miri, S. Hassan, Y. S. Zhang, *Adv. Mater.* **2018**, 30, 1805460.
- [156] M. Shin, K. H. Song, J. C. Burrell, D. K. Cullen, J. A. Burdick, *Adv. Sci.* **2019**, 6, 1901229.
- [157] G. Aguirre, A. Khouch, P. Taboada, K. Chougrani, V. Alard, L. Billon, *Polym. Chem.* **2018**, 9, 1155.
- [158] B. P. Binks, P. D. I. Fletcher, B. L. Holt, P. Beausoubre, K. Wong, *Phys. Chem. Chem. Phys.* **2010**, 12, 11954.
- [159] S. Tasoglu, E. Diller, S. Guven, M. Sitti, U. Demirci, *Nat. Commun.* **2014**, 5, 3124.
- [160] T. Watanabe, Y. Yokoyama, T. Hayakawa, in *2019 20th Int. Conf. on Solid-State Sensors, Actuators and Microsystems & Eurosensors XXXIII (TRANSDUCERS & EUROSENSORS XXXIII)*, IEEE, Piscataway, NJ **2019**, pp. 84–87.
- [161] Y. Cao, R. Mezzenga, *Nat. Food* **2020**, 1, 106.
- [162] M. Destribats, M. Rouvet, C. Gehin-Delval, C. Schmitt, B. P. Binks, *Soft Matter* **2014**, 10, 6941.
- [163] M. Kwok, G. Sun, T. Ngai, *Langmuir* **2019**, 35, 4205.
- [164] B. V. Slaughter, S. S. Khurshid, O. Z. Fisher, A. Khademhosseini, N. A. Peppas, *Adv. Mater.* **2009**, 21, 3307.
- [165] Y. Xu, D. Li, X. Wang, in *Organ Manufacturing*, Nova Science, NY, USA **2015**, p. 245.
- [166] Y.-J. Lin, F.-C. Hsu, C.-W. Chou, T.-H. Wu, H.-R. Lin, *J. Mater. Chem. B* **2014**, 2, 8329.
- [167] Y. Tanaka, J. P. Gong, Y. Osada, *Prog. Polym. Sci.* **2005**, 30, 1.
- [168] S. Berger, H. Zhang, A. Pich, *Adv. Funct. Mater.* **2009**, 19, 554.

- [169] M. E. Furth, A. Atala, M. E. Van Dyke, *Biomaterials* **2007**, 28, 5068.
- [170] J. E. Meiring, M. J. Schmid, S. M. Grayson, B. M. Rathasack, D. M. Johnson, R. Kirby, R. Kannappan, K. Manthiram, B. Hsia, Z. L. Hogan, A. D. Elington, M. V. Pishko, C. G. Willson, *Chem. Mater.* **2004**, 16, 5574.
- [171] A. S. Hoffman, *Adv. Drug Delivery Rev.* **2012**, 64, 18.
- [172] B. R. Saunders, B. Vincent, *Adv. Colloid Interface Sci.* **1999**, 80, 1.
- [173] D. Chen, E. Amstad, C. X. Zhao, L. Cai, J. Fan, Q. Chen, M. Hai, S. Koehler, H. Zhang, F. Liang, Z. Yang, D. A. Weitz, *ACS Nano* **2017**, 11, 11978.
- [174] E. Mei, S. Li, J. Song, R. Xing, Z. Li, X. Yan, *Colloids Surf., A* **2019**, 577, 570.
- [175] M. M. Stevens, R. P. Marini, D. Schaefer, J. Aronson, R. Langer, V. P. Shastri, *Proc. Natl. Acad. Sci. U. S. A.* **2005**, 102, 11450.
- [176] A. Kamada, A. Levin, Z. Toprakcioglu, Y. Shen, V. Lutz-Bueno, K. N. Baumann, P. Mohammadi, M. B. Linder, R. Mezzenga, T. P. J. Knowles, *Small* **2020**, 16, 1904190.
- [177] J. Glowacki, S. Mizuno, *Biopolymers* **2008**, 89, 338.
- [178] R. Xing, K. Liu, T. Jiao, N. Zhang, K. Ma, R. Zhang, Q. Zou, G. Ma, X. Yan, *Adv. Mater.* **2016**, 28, 3669.
- [179] J. L. Puetzer, T. Ma, I. Sallent, A. Gelmi, M. M. Stevens, *Biomaterials* **2021**, 269, 120527.
- [180] V. Lutz-Bueno, S. Bolisetty, P. Azzari, S. Handschin, R. Mezzenga, *Adv. Mater.* **2020**, 32, 2004941.
- [181] U. S. Pal, R. K. Singh, S. Mohammad, R. K. Yadav, *J. Maxillofac. Oral Surg.* **2009**, 8, 261.
- [182] D. Thomas, G. Fontana, X. Chen, C. Sanz-Nogués, D. I. Zeugolis, P. Dockery, T. O'Brien, A. Pandit, *Biomaterials* **2014**, 35, 8757.
- [183] L. Zhou, C. Ruiz-Puig, B.-A. Jacobs, X. Han, R. Lisle, H. Bayley, X. Lu, *Adv. Funct. Mater.* **2021**, 31, 2007514.
- [184] J. W. Nichol, S. T. Koshy, H. Bae, C. M. Hwang, S. Yamanlar, A. Khademhosseini, *Biomaterials* **2010**, 31, 5536.
- [185] A. I. Van Den Bulcke, B. Bogdanov, N. De Rooze, E. H. Schacht, M. Cornelissen, H. Berghmans, *Biomacromolecules* **2000**, 1, 31.
- [186] L. Ouyang, J. P. K. Armstrong, M. Salmeron-Sanchez, M. M. Stevens, *Adv. Funct. Mater.* **2020**, 30, 1909009.
- [187] K. Yue, G. Trujillo-de Santiago, M. M. Alvarez, A. Tamayol, N. Annabi, A. Khademhosseini, *Biomaterials* **2015**, 73, 254.
- [188] P. E. Ludwig, T. J. Huff, J. M. Zuniga, *J. Tissue Eng.* **2018**, 9, 204173141876986.
- [189] X. Zhao, S. Liu, L. Yildirim, H. Zhao, R. Ding, H. Wang, W. Cui, D. Weitz, *Adv. Funct. Mater.* **2016**, 26, 2809.
- [190] Y. Fang, Y. Guo, M. Ji, B. Li, Y. Guo, J. Zhu, T. Zhang, Z. Xiong, *Adv. Funct. Mater.* **2022**, 32, 2109810.
- [191] N. Chai, J. Zhang, Q. Zhang, H. Du, X. He, J. Yang, X. Zhou, J. He, C. He, *Composites, Part B* **2021**, 223, 109100.
- [192] A. J. Seymour, S. Shin, S. C. Heilshorn, *Adv. Healthcare Mater.* **2021**, 10, 2100644.
- [193] L. Shao, Q. Gao, C. Xie, J. Fu, M. Xiang, Z. Liu, L. Xiang, Y. He, *Bio-Des. Manuf.* **2020**, 3, 30.
- [194] R. K. Birla, G. H. Borschel, R. G. Dennis, D. L. Brown, *Tissue Eng.* **2005**, 11, 803.
- [195] S.-W. Cho, I. Kim, S.-H. Kim, J. W. Rhie, C. Y. Choi, B.-S. Kim, *Biochem. Biophys. Res. Commun.* **2006**, 345, 588.
- [196] M. Alaminos, M. D. C. Sánchez-Quevedo, J. I. Muñoz-Ávila, D. Serrano, S. Medialdea, I. Carreras, A. Campos, *Invest. Ophthalmol. Visual Sci.* **2006**, 47, 3311.
- [197] Q. Ye, G. Zünd, P. Benedikt, S. Jockenhoevel, S. P. Hoerstrup, S. Sakyama, J. A. Hubbell, M. Turina, *Eur. J. Cardio-Thoracic Surg.* **2000**, 17, 587.
- [198] B. Derby, *Science* **2012**, 338, 921.
- [199] Y. Xu, D. Li, X. Wang, in *Organ Manufacturing*, Nova Science, NY, USA **2015**, pp. 101–125.
- [200] Y. Xu, D. Li, X. Wang, in *Organ Manufacturing*, Nova Science, NY, USA **2015**, pp. 201–225.
- [201] X. Zhao, L. Liu, J. Wang, Y. Xu, W. Zhang, G. Khang, X. Wang, *J. Tissue Eng. Regener. Med.* **2016**, 10, 833.
- [202] A. Tocchio, N. G. Durmus, K. Sridhar, V. Mani, B. Coskun, R. El Assal, U. Demirci, *Adv. Mater.* **2018**, 30, 1705034.
- [203] Y. Xu, X. Wang, *Biotechnol. Bioeng.* **2015**, 112, 1683.
- [204] M. Guthold, W. Liu, E. A. Sparks, L. M. Jawerth, L. Peng, M. Falvo, R. Superfine, R. R. Hantgan, S. T. Lord, *Cell Biochem. Biophys.* **2007**, 49, 165.
- [205] G. Chaudhary, A. Ghosh, N. A. Bharadwaj, J. G. Kang, P. V. Braun, K. S. Schweizer, R. H. Ewoldt, *Macromolecules* **2019**, 52, 3029.
- [206] Y. Shi, X. Gao, L. Chen, M. Zhang, J. Ma, X. Zhang, J. Qin, *Microfluid. Nanofluid.* **2013**, 15, 467.
- [207] M. Schindler, D. Siriwardena, T. N. Kohler, A. L. Ellermann, E. Slatery, C. Munger, F. Hollfelder, T. E. Boroviak, *Stem Cell Reports* **2021**, 16, 1347.
- [208] J. O. Jeppson, C. B. Laurell, B. Franzén, *Clin. Chem.* **1979**, 25, 629.
- [209] E. Mercey, P. Obeid, D. Glaize, M. L. Calvo-Muñoz, C. Guguen-Guillouzo, B. Fouqué, *Biomaterials* **2010**, 31, 3156.
- [210] H. Park, K. Park, W. S. W. Shalaby, *Biodegradable Hydrogels for Drug Delivery*, CRC Press, Boca Raton, FL **1993**.
- [211] A. Forget, R.-A. Pique, V. Ahmadi, S. Lüdeke, V. P. Shastri, *Macromol. Rapid Commun.* **2015**, 36, 196.
- [212] E. Tumarkin, L. Tzadu, E. Csaszar, M. Seo, H. Zhang, A. Lee, R. Peerani, K. Purpura, P. W. Zandstra, E. Kumacheva, *Integr. Biol.* **2011**, 3, 653.
- [213] S. Liang, J. Xu, L. Weng, H. Dai, X. Zhang, L. Zhang, *J. Controlled Release* **2006**, 115, 189.
- [214] L. Liu, C. K. Dalal, B. M. Heineke, A. R. Abate, *Lab Chip* **2019**, 19, 1838.
- [215] H. Iwata, K. Kobayashi, T. Takagi, T. Oka, H. Yang, H. Amemiya, T. Tsuji, F. Ito, *J. Biomed. Mater. Res.* **1994**, 28, 1003.
- [216] X.-M. Zhou, U. Shimanovich, T. W. Herling, S. Wu, C. M. Dobson, T. P. J. Knowles, S. Perrett, *ACS Nano* **2015**, 9, 5772.
- [217] X. Liu, Z. Toprakcioglu, A. J. Dear, A. Levin, F. S. Ruggeri, C. G. Taylor, M. Hu, J. R. Kumita, M. Andreasen, C. M. Dobson, U. Shimanovich, T. P. J. Knowles, *Macromol. Rapid Commun.* **2019**, 40, 1800898.
- [218] S. Zilberzwige-Tal, E. Gazit, *Chem. - Asian J.* **2018**, 13, 3437.
- [219] Z. A. Arnon, S. Gilead, E. Gazit, *Nanotechnology* **2019**, 30, 102001.
- [220] U. Shimanovich, I. Efimov, T. O. Mason, P. Flagmeier, A. K. Buell, A. Gedanken, S. Linse, K. S. Åkerfeldt, C. M. Dobson, D. A. Weitz, T. P. J. Knowles, *ACS Nano* **2015**, 9, 43.
- [221] C. Yuan, W. Ji, R. Xing, J. Li, E. Gazit, X. Yan, *Nat. Rev. Chem.* **2019**, 3, 567.
- [222] S. Ling, D. L. Kaplan, M. J. Buehler, *Nat. Rev. Mater.* **2018**, 3, 18016.
- [223] Y. Wang, J. Guo, L. Zhou, C. Ye, F. G. Omenetto, D. L. Kaplan, S. Ling, *Adv. Funct. Mater.* **2018**, 28, 1805305.
- [224] T. O. Mason, U. Shimanovich, *Adv. Mater.* **2018**, 30, 1706462.
- [225] L. W. Y. Roode, U. Shimanovich, S. Wu, S. Perrett, T. P. J. Knowles, *Biological and Bio-inspired Nanomaterials*, Vol. 1174, Springer, Singapore **2019**, p. 223.
- [226] A. Zbinden, M. Pérez-Berlangua, P. De Rossi, M. Polymenidou, *Dev. Cell* **2020**, 55, 45.
- [227] Y. Lin, Y. Fichou, Z. Zeng, N. Y. Hu, S. Han, *ACS Chem. Neurosci.* **2020**, 11, 615.
- [228] J. S. Kahn, R. C. H. Ruiz, S. Sureka, S. Peng, T. L. Derrien, D. An, D. Luo, *Biomacromolecules* **2016**, 17, 2019.
- [229] F. Li, D. Lyu, S. Liu, W. Guo, *Adv. Mater.* **2020**, 32, 1806538.
- [230] C. Li, A. Faulkner-Jones, A. R. Dun, J. Jin, P. Chen, Y. Xing, Z. Yang, Z. Li, W. Shu, D. Liu, R. R. Duncan, *Angew. Chem., Int. Ed.* **2015**, 54, 3957.

- [231] C. A. Hong, J. S. Kim, S. H. Lee, W. H. Kong, T. G. Park, H. Mok, Y. S. Nam, *Adv. Funct. Mater.* **2013**, 23, 316.
- [232] J. Li, C. Zheng, S. Cansiz, C. Wu, J. Xu, C. Cui, Y. Liu, W. Hou, Y. Wang, L. Zhang, I. Teng, H. Yang, W. Tan, *J. Am. Chem. Soc.* **2015**, 137, 1412.
- [233] H. Ahmed, B. T. Stokke, *Lab Chip* **2021**, 21, 2232.
- [234] C. Moraes, A. B. Simon, A. J. Putnam, S. Takayama, *Biomaterials* **2013**, 34, 9623.
- [235] J. He, M. Mao, Y. Liu, J. Shao, Z. Jin, D. Li, *Adv. Healthcare Mater.* **2013**, 2, 1108.
- [236] M. Meier, J. Kennedy-Darling, S. H. Choi, E. M. Norstrom, S. S. Sisodia, R. F. Ismagilov, *Angew. Chem.* **2009**, 121, 1515.
- [237] M. Lian, C. P. Collier, M. J. Doktycz, S. T. Retterer, *Biomicrofluidics* **2012**, 6, 044108.
- [238] H. Shieh, M. Saadatmand, M. Eskandari, D. Bastani, *Sci. Rep.* **2021**, 11, 1565.
- [239] R. K. Shah, J.-W. Kim, J. J. Agresti, D. A. Weitz, L.-Y. Chu, *Soft Matter* **2008**, 4, 2303.
- [240] Y. Song, U. Shimanovich, T. C. T. Michaels, Q. Ma, J. Li, T. P. J. Knowles, H. C. Shum, *Nat. Commun.* **2016**, 7, 12934.
- [241] Y. Song, Y. K. Chan, Q. Ma, Z. Liu, H. C. Shum, *ACS Appl. Mater. Interfaces* **2015**, 7, 13925.
- [242] Y. Li, P. Chen, Y. Wang, S. Yan, X. Feng, W. Du, S. A. Koehler, U. Demirci, B.-F. Liu, *Adv. Mater.* **2016**, 28, 3543.
- [243] H. Zhang, L. Koens, E. Lauga, A. Mourran, M. Möller, *Small* **2019**, 15, 1903379.
- [244] H. Qi, M. Ghodousi, Y. Du, C. Grun, H. Bae, P. Yin, A. Khademhosseini, *Nat. Commun.* **2013**, 4, 2275.
- [245] H. Zhou, X. Sun, L. Zhang, P. Zhang, J. Li, Y.-N. Liu, *Langmuir* **2012**, 28, 14553.
- [246] S. Ray, N. Singh, R. Kumar, K. Patel, S. Pandey, D. Datta, J. Mahato, R. Panigrahi, A. Navalkar, S. Mehra, L. Gadhe, D. Chatterjee, A. S. Sawner, S. Maiti, S. Bhatia, J. A. Gerez, A. Chowdhury, A. Kumar, R. Padinhateeri, R. Riek, G. Krishnamoorthy, S. K. Maji, *Nat. Chem.* **2020**, 12, 705.
- [247] M. G. F. Last, S. Deshpande, C. Dekker, *ACS Nano* **2020**, 14, 4487.
- [248] K. Chen, T. J. Merkel, A. Pandya, M. E. Napier, J. C. Luft, W. Daniel, S. Sheiko, J. M. DeSimone, *Biomacromolecules* **2012**, 13, 2748.
- [249] J. L. Perry, K. P. Herlihy, M. E. Napier, J. M. Desimone, *Acc. Chem. Res.* **2011**, 44, 990.
- [250] K. Chen, J. Xu, J. C. Luft, S. Tian, J. S. Raval, J. M. DeSimone, *J. Am. Chem. Soc.* **2014**, 136, 9947.
- [251] M. L. Eggersdorfer, H. Seybold, A. Ofner, D. A. Weitz, A. R. Studart, *Proc. Natl. Acad. Sci. U. S. A.* **2018**, 115, 9479.
- [252] E. Stolovicki, R. Ziblat, D. A. Weitz, *Lab Chip* **2018**, 18, 132.
- [253] T. Nisisako, T. Ando, T. Hatsuzawa, *Small* **2014**, 10, 5116.
- [254] C. Li, L. Ouyang, J. P. K. Armstrong, M. M. Stevens, *Trends Biotechnol.* **2021**, 39, 150.
- [255] Y. Zhang, M. A. Wright, K. L. Saar, P. Challa, A. S. Morgunov, Q. A. E. Peter, S. Devenish, C. M. Dobson, T. P. J. Knowles, *Lab Chip* **2021**, 21, 2922.
- [256] Y. Xia, G. M. Whitesides, *Annu. Rev. Mater. Sci.* **1998**, 28, 153.
- [257] J. G. Werner, S. Nawar, A. A. Solovev, D. A. Weitz, *Macromolecules* **2018**, 51, 5798.
- [258] M. Samandari, F. Alipanah, S. H. Javanmard, A. Sanati-Nezhad, *Sens. Actuators, B* **2019**, 291, 418.
- [259] K. Ren, W. Dai, J. Zhou, J. Su, H. Wu, *Proc. Natl. Acad. Sci. USA* **2011**, 108, 8162.
- [260] M. Tenje, F. Cantoni, A. M. Porras Hernández, S. S. Searle, S. Johansson, L. Barbe, M. Antfolk, H. Pohlitz, *Organs-on-a-Chip* **2020**, 2, 100003.
- [261] B. G. Chung, K.-H. Lee, A. Khademhosseini, S.-H. Lee, *Lab Chip* **2012**, 12, 45.
- [262] U. Shimanovich, D. Pinotsi, K. Shimanovich, N. Yu, S. Bolisetty, J. Adamcik, R. Mezzenga, J. Charmet, F. Vollrath, E. Gazit, C. M. Dobson, G. K. Schierle, C. Holland, C. F. Kaminski, T. P. J. Knowles, *Macromol. Biosci.* **2018**, 18, 1700295.
- [263] J.-T. Wang, J. Wang, J.-J. Han, *Small* **2011**, 7, 1728.
- [264] D. C. Duffy, J. C. McDonald, O. J. A. Schueller, G. M. Whitesides, *Anal. Chem.* **1998**, 70, 4974.
- [265] K. Liu, H.-J. Ding, J. Liu, Y. Chen, X.-Z. Zhao, *Langmuir* **2006**, 22, 9453.
- [266] L. B. Zhao, L. Pan, K. Zhang, S. S. Guo, W. Liu, Y. Wang, Y. Chen, X. Z. Zhao, H. L. W. Chan, *Lab Chip* **2009**, 9, 2981.
- [267] J.-W. Kim, A. S. Utada, A. Fernández-Nieves, Z. Hu, D. A. Weitz, *Angew. Chem.* **2007**, 119, 1851.
- [268] L.-Y. Chu, A. S. Utada, R. K. Shah, J.-W. Kim, D. A. Weitz, *Angew. Chem.* **2007**, 119, 9128.
- [269] L.-Y. Chu, J.-W. Kim, R. K. Shah, D. A. Weitz, *Adv. Funct. Mater.* **2007**, 17, 3499.
- [270] Y. Song, T. C. T. Michaels, Q. Ma, Z. Liu, H. Yuan, S. Takayama, T. P. J. Knowles, H. C. Shum, *Nat. Commun.* **2018**, 9, 2110.
- [271] S. Park, H. J. Lee, W.-G. Koh, *Sensors* **2012**, 12, 8426.
- [272] D. Poncelet, R. Lencki, C. Beaulieu, J. P. Halle, R. J. Neufeld, A. Fournier, *Appl. Microbiol. Biotechnol.* **1992**, 38, 39.
- [273] C. G. De Kruijff, F. Weinbreck, R. de Vries, *Curr. Opin. Colloid Interface Sci.* **2004**, 9, 340.
- [274] A. Ianiro, H. Wu, M. M. J. van Rijt, M. P. Vena, A. D. A. Keizer, A. C. C. Esteves, R. Tuinier, H. Friedrich, N. A. J. M. Sommerdijk, J. P. Patterson, *Nat. Chem.* **2019**, 11, 320.
- [275] H.-J. Jin, D. L. Kaplan, *Nature* **2003**, 424, 1057.
- [276] C. Cha, J. Oh, K. Kim, Y. Qiu, M. Joh, S. R. Shin, X. Wang, G. Camci-Unal, K. Wan, R. Liao, A. Khademhosseini, *Biomacromolecules* **2014**, 15, 283.
- [277] B. Haney, J. G. Werner, D. A. Weitz, S. Ramakrishnan, *ACS Appl. Mater. Interfaces* **2020**, 12, 33439.
- [278] P.-H. Kim, H.-G. Yim, Y.-J. Choi, B.-J. Kang, J. Kim, S.-M. Kwon, B.-S. Kim, N. S. Hwang, J.-Y. Cho, *J. Controlled Release* **2014**, 187, 1.
- [279] S. Hou, R. Lake, S. Park, S. Edwards, C. Jones, K. J. Jeong, *ACS Appl. Bio Mater.* **2018**, 1, 1430.
- [280] T. J. Merkel, K. P. Herlihy, J. Nunes, R. M. Orgel, J. P. Rolland, J. M. DeSimone, *Langmuir* **2010**, 26, 13086.
- [281] C. Holtze, A. C. Rowat, J. J. Agresti, J. B. Hutchison, F. E. Angile, C. H. J. Schmitz, S. Köster, H. Duan, K. J. Humphry, R. A. Scanga, J. S. Johnson, D. Pisignano, D. A. Weitz, *Lab Chip* **2008**, 8, 1632.
- [282] S. Tian, Z. Zhang, J. Chen, M. Du, Z. Li, H. Yang, X. Ji, Z. He, *Talanta* **2018**, 186, 24.
- [283] N. M. Kovalchuk, A. Trybala, V. Starov, O. Matar, N. Ivanova, *Adv. Colloid Interface Sci.* **2014**, 210, 65.
- [284] A. Domínguez, A. Fernández, N. González, E. Iglesias, L. Montenegro, *J. Chem. Educ.* **1997**, 74, 1227.
- [285] B. Wedel, T. Brändel, J. Bookhold, T. Hellweg, *ACS Omega* **2017**, 2, 84.
- [286] A. Alcinesio, O. J. Meacock, R. G. Allan, C. Monico, V. R. Schild, I. Cazimoglu, M. T. Cornall, R. K. Kumar, H. Bayley, *Nat. Commun.* **2020**, 11, 2105.
- [287] O. Wagner, J. Thiele, M. Weinhart, L. Mazutis, D. A. Weitz, W. T. S. Huck, R. Haag, *Lab Chip* **2016**, 16, 65.
- [288] T. F. Tadros, *Applied Surfactants: Principles and Applications*, Wiley-VCH, Weinheim **2005**, 1.
- [289] T. F. Tadros, *Applied Surfactants: Principles and Applications*, Wiley-VCH, Weinheim **2005**, 73.
- [290] P. Raychaudhuri, Q. Li, A. Mason, E. Mikhailova, A. J. Heron, H. Bayley, *Biochemistry* **2011**, 50, 1599.
- [291] G. Villar, A. D. Graham, H. Bayley, *Science* **2013**, 340, 48.
- [292] M. Hua, Y. Du, J. Song, M. Sun, X. He, *J. Mater. Res.* **2019**, 34, 206.
- [293] C. Kim, K. S. Lee, Y. E. Kim, K.-J. Lee, S. H. Lee, T. S. Kim, J. Y. Kang, *Lab Chip* **2009**, 9, 1294.
- [294] C. Kim, S. Chung, Y. E. Kim, K. S. Lee, S. H. Lee, K. W. Oh, J. Y. Kang, *Lab Chip* **2011**, 11, 246.

- [295] R. K. Shah, J.-W. Kim, D. A. Weitz, *Langmuir* **2010**, 26, 1561.
- [296] Y. M. Ye, M. Nishi, W. Q. Yang, M. Takinoue, N. Miyamoto, *Key Eng. Mater.* **2019**, 804, 75.
- [297] S. Damiani, *Macromol. Res.* **2020**, 28, 1046.
- [298] L. Zhou, A. C. Wolfes, Y. Li, D. C. W. Chan, H. Ko, F. G. Szele, H. Bayley, *Adv. Mater.* **2020**, 32, 2002183.
- [299] M. Karbaschi, P. Shahi, A. R. Abate, *Biomicrofluidics* **2017**, 11, 044107.
- [300] J. Ayarza, Y. Coello, J. Nakamatsu, *Int. J. Polym. Anal. Charact.* **2017**, 22, 1.
- [301] L. Schnaider, Z. Toprakcioglu, A. Ezra, X. Liu, D. Bychenko, A. Levin, E. Gazit, T. P. J. Knowles, *Nano Lett.* **2020**, 20, 1590.
- [302] K. Geisel, K. Henzler, P. Guttman, W. Richtering, *Langmuir* **2015**, 31, 83.
- [303] A. Späth, B. A. Graf-Zeiler, G. Paradossi, S. Ghugare, G. Tzvetkov, R. H. Fink, *RSC Adv.* **2016**, 6, 98228.
- [304] R. Keidel, A. Ghavami, D. M. Lugo, G. Lotze, O. Virtanen, P. Beumers, J. S. Pedersen, A. Bardow, R. G. Winkler, W. Richtering, *Sci. Adv.* **2018**, 4, eaao7086.
- [305] S. Nöjd, P. Holmqvist, N. Boon, M. Obiols-Rabasa, P. S. Mohanty, R. Schweins, P. Schurtenberger, *Soft Matter* **2018**, 14, 4150.
- [306] P. S. Mohanty, S. Nöjd, K. van Gruijthuisen, J. J. Crassous, M. Obiols-Rabasa, R. Schweins, A. Stradner, P. Schurtenberger, *Sci. Rep.* **2017**, 7, 1487.
- [307] A. C. Nickel, A. Scotti, J. E. Houston, T. Ito, J. Crassous, J. S. Pedersen, W. Richtering, *Nano Lett.* **2019**, 19, 8161.
- [308] A. Scotti, A. R. Denton, M. Brugnoli, J. E. Houston, R. Schweins, I. I. Potemkin, W. Richtering, *Macromolecules* **2019**, 52, 3995.
- [309] J. A. Allegretto, J. M. Giusti, S. E. Moya, O. Azzaroni, M. Rafti, *RSC Adv.* **2020**, 10, 2453.
- [310] A. P. M. Guttenplan, *Ph.D. Smart Nanomaterials from Repeat Proteins and Amyloid Fibrils*, University of Cambridge, **2018**.
- [311] L. R. Volpatti, U. Shimanovich, F. S. Ruggeri, S. Bolisetty, T. Müller, T. O. Mason, T. C. T. Michaels, R. Mezzenga, G. Dietler, T. P. J. Knowles, *J. Mater. Chem. B* **2016**, 4, 7989.
- [312] Y. Li, O. S. Sar-iyer, A. Ramachandran, S. Panyukov, M. Rubinstein, E. Kumacheva, *Sci. Rep.* **2015**, 5, 17017.
- [313] Y. Li, J. M. Kleijn, M. A. C. Stuart, T. Slaghek, J. Timmermans, W. Norde, *Soft Matter* **2011**, 7, 1926.
- [314] F. Di Lorenzo, S. Seiffert, *Macromolecules* **2013**, 46, 1962.
- [315] S. Fujii, S. P. Armes, T. Araki, H. Ade, *J. Am. Chem. Soc.* **2005**, 127, 16808.
- [316] M. Tayebi, Y. Zhou, P. Tripathi, R. Chandramohanadas, Y. Ai, *Anal. Chem.* **2020**, 92, 10733.
- [317] W. Lei, C. Xie, T. Wu, X. Wu, M. Wang, *Sci. Rep.* **2019**, 9, 1453.
- [318] C. C. L. Schuurmans, A. Abbadesse, M. A. Bengtson, G. Pletikapic, H. B. Eral, G. Koenderink, R. Masereeuw, W. E. Hennink, T. Vermonden, *Soft Matter* **2018**, 14, 6327.
- [319] D. W. Sanders, N. Kedersha, D. S. W. Lee, A. R. Strom, V. Drake, J. A. Riback, D. Bracha, J. M. Eeftens, A. Iwanicki, A. Wang, M. Wei, G. Whitney, S. M. Lyons, P. Anderson, W. M. Jacobs, P. Ivanov, C. P. Brangwynne, *Cell* **2020**, 181, 306.
- [320] R. Subbiah, C. Hipfinger, A. Tahayeri, A. Athirasala, S. Horsophonphong, G. Thirivikraman, C. M. França, D. A. Cunha, A. Mansoorifar, A. Zahariev, J. M. Jones, P. G. Coelho, L. Witek, H. Xie, R. E. Guldborg, L. E. Bertassoni, *Adv. Mater.* **2020**, 32, 2001736.
- [321] A. Palika, A. Armanious, A. Rahimi, C. Medaglia, M. Gasbarri, S. Handschin, A. Rossi, M. O. Pohl, I. Busnadiego, R. B. Anjanappa, S. Bolisetty, M. Peydayesh, S. Stertz, B. G. Hale, C. Tapparel, F. Stellacci, R. Mezzenga, *Nat. Nanotechnol.* **2021**, 16, 918.
- [322] E. Amstad, M. Chemama, M. Eggersdorfer, L. R. Arriaga, M. P. Brenner, D. A. Weitz, *Lab Chip* **2016**, 16, 4163.
- [323] R. Feng, L. Wang, P. Zhou, Z. Luo, X. Li, L. Gao, *Carbohydr. Polym.* **2020**, 250, 116917.
- [324] E. Yammine, E. Souaid, S. Youssef, M. Abboud, S. Mornet, M. Nakhl, E. Duguet, *Part. Part. Syst. Charact.* **2020**, 37, 2000111.
- [325] D. Husman, P. B. Welzel, S. Vogler, L. J. Bray, N. Träber, J. Friedrichs, V. Körber, M. V. Tsurkan, U. Freudenberger, J. Thiele, C. Werner, *Biomater. Sci.* **2020**, 8, 101.
- [326] Z. Tu, W. Liu, J. Wang, X. Qiu, J. Huang, J. Li, H. Lou, *Nat. Commun.* **2021**, 12, 2916.
- [327] X. Kuang, S. Wu, Q. Ze, L. Yue, Y. Jin, S. M. Montgomery, F. Yang, H. J. Qi, R. Zhao, *Adv. Mater.* **2021**, 33, 2102113.
- [328] M. M. Alvarez, J. Aizenberg, M. Analoui, A. M. Andrews, G. Bisker, E. S. Boyden, R. D. Kamm, J. M. Karp, D. J. Mooney, R. Oklu, Dan Peer, M. Stolzoff, M. S. Strano, G. T. Santiago, T. J. Webster, P. S. Weiss, A. Khademhosseini, *ACS Nano* **2017**, 11, 5195.
- [329] Y. Chen, J. Huang, R. Chen, L. Yang, J. Wang, B. Liu, L. Du, Y. Yi, J. Jia, Y. Xu, Q. Chen, D. G. Ngondi, Y. Miao, Z. Hu, *Theranostics* **2020**, 10, 1454.
- [330] U. Kauscher, M. N. Holme, M. Björnmalin, M. M. Stevens, *Adv. Drug Delivery Rev.* **2019**, 138, 259.
- [331] S. Peng, F. Cao, Y. Xia, X.-D. Gao, L. Dai, J. Yan, G. Ma, *Adv. Mater.* **2020**, 32, 2004210.
- [332] H. Meng, P. K. Forooshani, P. U. Joshi, J. Osborne, X. Mi, C. Meingast, R. Pinnaratip, J. Kelley, A. Narkar, W. He, M. C. Frost, C. L. Heldt, B. P. Lee, *Acta Biomater.* **2019**, 83, 109.
- [333] F. Narita, Z. Wang, H. Kurita, Z. Li, Y. Shi, Y. Jia, C. Soutis, *Adv. Mater.* **2021**, 33, 2005448.
- [334] M. Peydayesh, R. Mezzenga, *Nat. Commun.* **2021**, 12, 3248.
- [335] A. M. Duraj-Thatte, A. Manjula-Basavanna, N.-M. D. Courchesne, G. I. Cannici, A. Sánchez-Ferrer, B. P. Frank, L. van't Hag, S. K. Cotts, D. H. Fairbrother, R. Mezzenga, N. S. Joshi, *Nat. Chem. Biol.* **2021**, 17, 732.
- [336] A. J. Najibi, D. J. Mooney, *Adv. Drug Delivery Rev.* **2020**, 161, 42.
- [337] T. M. Caputo, A. Cummaro, V. Lettera, A. Mazzarotta, E. Battista, P. A. Netti, F. Causa, *Analyst* **2019**, 144, 1369.
- [338] T. F. Tadros, *Applied Surfactants: Principles and Applications*, Wiley-VCH, Weinheim **2005**, 1.
- [339] A. W. P. Fitzpatrick, G. T. Debelouchina, M. J. Bayro, D. K. Clare, M. A. Caporini, V. S. Bajaj, C. P. Jaroniec, L. Wang, V. Ladizhansky, S. A. Müller, C. E. MacPhee, C. A. Waudby, H. R. Mott, A. De Simone, T. P. J. Knowles, H. R. Saibil, M. Vendruscolo, E. V. Orlova, R. G. Griffin, C. M. Dobson, *Proc. Natl. Acad. Sci. USA* **2013**, 110, 5468.
- [340] S. C. Santos, C. A. Custódio, J. F. Mano, *Adv. Healthc. Mater.* **2018**, 7, 1800849.
- [341] N. D. Dinh, M. Kukumberg, A. T. Nguyen, H. Keramati, S. Guo, D. T. Phan, N. B. Ja'afar, E. Birgersson, H. L. Leo, R. Y. Huang, T. Kofidis, A. J. Rufaihah, C. H. Chen, *Lab Chip* **2020**, 20, 2756.



**Yi Shen** joined University of Sydney as a lecturer in the School of Chemical and Biomolecular Engineering since September 2020. Her research interests span from biophysics to material science with a focus on protein phase behavior by exploiting a set of soft matter approaches and microfluidic techniques. Prior to this position, she was a postdoc in the Chemistry Department, Centre for Misfolding Diseases at the University of Cambridge from 2018 to 2020. She obtained her Ph.D. degree in 2017 from the Department of Health Sciences and Technology at ETH Zurich. Before her Ph.D., she also worked with Prof. Howard Stone at Princeton University on bio-microfluidics.



**Tuomas P. J. Knowles** is professor of physical chemistry and biophysics at Cambridge University. He received his undergraduate degree in physics from ETH Zurich, and a Ph.D. in biological physics from the University of Cambridge. He was then a St. John's College research fellow working at Cambridge University and Harvard University, and joined the faculty of the Cambridge Department of Chemistry in 2010. His research focuses on the development and application of experimental and theoretical methods from the physical sciences for the study of biomolecular behavior and interactions in the context of biological function and malfunction.